Evaluation of the transition to steady state in somatosensory evoked potentials (SEPs) as a response to increasing stimulation frequency

MSc Thesis

Zoe Centeno Sanz

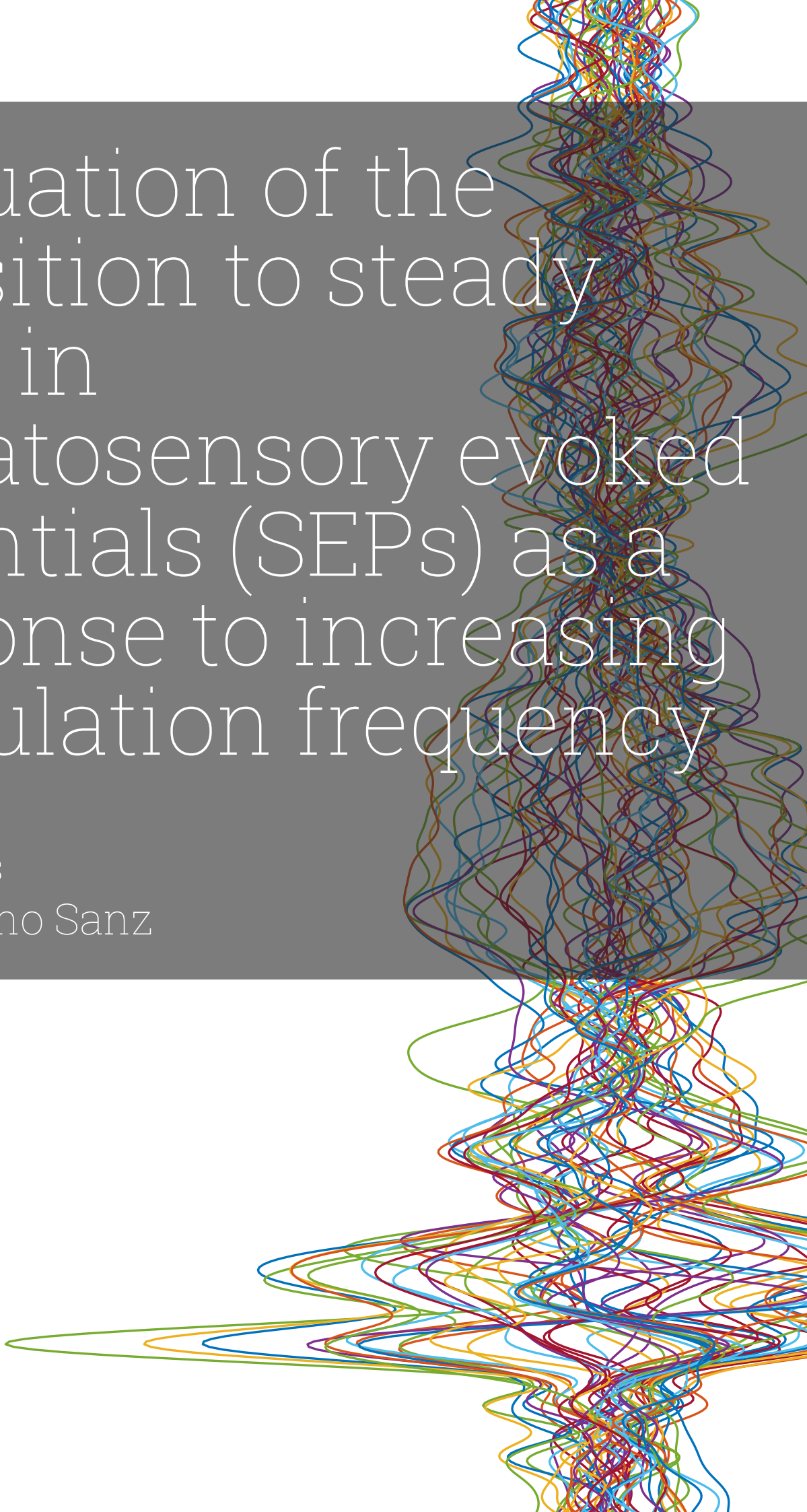

Evaluation of the transition to steady state in somatosensory evoked potentials (SEPs) as a response to increasing stimulation frequency

by

Zoe Centeno Sanz

In partial fulfilment of the requirements for the degree of:
Master of Science
in Mechanical Engineering

at the Delft University of Technology,
to be defended publicly on Friday September 26, 2025 at 13:30 h

Supervisor:	Dr. Mark van de Ruit
Daily supervisor:	Ioannis Kyriazis
Thesis committee:	Dr. Mark van de Ruit
	Dr. Matin Jafarian
	Dr. Jason K. Moore

TU Delft

Acknowledgements

As I write these words, my mind goes back to two years ago, when I was writing the acknowledgements section of my bachelor's thesis. While my bachelor years were filled with exploration and discovery, I can say that these two years have been a source of knowledge and confidence. I am grateful to the many people who have contributed to my completion of this master in a direct or indirect way.

I would first like to thank my supervisors Mark and Ioannis for their guidance, support and kindness. I have learned a lot through this project, and this is partly thanks to their supervision. I have also felt that my ideas were valued, and this is greatly due to their supervision. I also feel grateful towards all the friends I made in Delft. This journey would have looked very different if they had not been part of it, and I can only smile looking back at what we have lived together during these two years.

Then, I would like to thank my close friends from Madrid. Even though they have not been involved in this project, our friendship irradiates a positive energy which contributes to everything I do, including this thesis. A special thank you goes to my father, my mother and my brother, for supporting me during this phase as they have always done, and to Borja for making everything feel simple.

Because the end of this master's thesis marks a halt (at least for now) in my academic trajectory, I would like to thank the many dedicated professors and teachers who have contributed to my education so far, for fueling my desire to always continue learning.

Zoe Centeno Sanz
Delft, September 2025

Abstract

Electrical stimulation of the median nerve is known to activate somatosensory pathways and elicit somatosensory-evoked potentials (SEPs), measurable with the electroencephalogram (EEG). In contrast to the traditional stimulation with individual pulses, alternative approaches indicate that periodic pulses may elicit, at some frequencies of stimulation, a steady-state SEP in which the dominant frequency of the EEG corresponds with that of the stimulation. Even though this steady-state approach presents several practical benefits and it may enable new applications, its study in the somatosensory system has been limited so far, especially with electrical stimulation.

To bridge this gap, this study aimed to identify measurable changes in the brain response to periodic electrical stimulation when stimulation frequency is increased, as well as to identify a potential threshold frequency at which the steady state appears.

With this purpose, transcutaneous electrical stimulation was used to stimulate the median nerve of 9 healthy subjects using pulse trains with frequencies of 3, 7, 13, 19 and 36 Hz. Time and frequency domain analyses were used to compare responses across all stimulation frequencies.

Results of the analysis in the time domain showed a significant decrease in the amplitude of SEP component P40 for the highest frequencies (19 and 36 Hz) compared to the lowest frequency (3 Hz), as well as a maximal activation centered at the somatosensory cortex, contralateral to the stimulated side. Results of analysis in the frequency domain showed salient peaks in the frequency spectra at the frequencies of 19 and 36 Hz, which were not present for the lower frequencies. Additionally, the power distribution across the scalp at these frequencies showed higher values at the side contralateral to the stimulation.

According to previous definitions of a steady-state in evoked potentials, our results indicate that a steady-state SEP can be elicited by transcutaneous electrical stimulation at frequencies of 19 Hz and above. These observations could be interpreted as a transition in the nature of the response due to the activation of neural pathways different to those activated for lower frequencies. However, further research is needed to confirm this hypothesis.

Contents

Evaluation of the transition to steady state in somatosensory evoked potentials (SEPs) as a response to increasing stimulation frequency

Zoe Centeno Sanz (6069142)
zcenteno@tudelft.nl

***Abstract*—Electrical stimulation of the median nerve is known to activate somatosensory pathways and elicit somatosensory evoked potentials (SEPs), measurable with the electroencephalogram (EEG). In contrast to the traditional stimulation with individual pulses, alternative approaches indicate that periodic pulses may elicit, at some frequencies of stimulation, a steady-state SEP in which the dominant frequency of the EEG corresponds with that of the stimulation. Even though this steady-state approach presents several practical benefits and it may enable new applications, its study in the somatosensory system has been limited so far, especially with electrical stimulation. To bridge this gap, this study aimed to identify measurable changes in the brain response to periodic electrical stimulation when stimulation frequency is increased, as well as to identify a potential threshold frequency at which the steady state appears. With this purpose, transcutaneous electrical stimulation was used to stimulate the median nerve of 9 healthy subjects using pulse trains with frequencies of 3, 7, 13, 19 and 36 Hz. Time and frequency domain analyses were used to compare responses across all stimulation frequencies. Results of the analysis in the time domain showed a significant decrease in the amplitude of SEP component P40 for the highest frequencies (19 and 36 Hz) compared to the lowest frequency (3 Hz), as well as a maximal activation centered at the somatosensory cortex, contralateral to the stimulated side. Results of analysis in the frequency domain showed salient peaks in the frequency spectra at the frequencies of 19 and 36 Hz, which were not present for the lower frequencies. Additionally, the power distribution across the scalp at these frequencies showed higher values at the side contralateral to the stimulation. According to previous definitions of a steady-state in evoked potentials, our results indicate that a steady-state SEP can be elicited by transcutaneous electrical stimulation at frequencies of 19 Hz and above. These observations could be interpreted as a transition in the nature of the response due to the activation of neural pathways different to those activated for lower frequencies. However, further research is needed to confirm this hypothesis.**

***Index Terms*—EEG, somatosensory evoked potential, SEP, steady state, electrical stimulation, Fourier transform**

I. Introduction

A somatosensory evoked potential (SEP) is the electrical activity of the nervous system that results from the stimulation of somatosensory pathways, which are those related to perception of touch, pressure and vibration. When this electrical activity reaches the outer layers of the cortex, it can be detected with the electroencephalogram (EEG), a non-invasive technique that measures the electrical potential difference between several points in the surface of the scalp.

Somatosensory pathways can be activated by electrical stimulation of the afferent fibres in the peripheral nervous system through the skin, for example the median nerve, which can be stimulated at the wrist. Electrical stimulation allows to finely tune the frequency, amplitude and duration of the delivered stimuli. Measurement of SEPs with EEG is a common procedure to investigate transmission and processing of stimuli in the peripheral and central nervous systems as part of the diagnosis and monitoring of neuropathologies, as well as for intraoperative monitoring to evaluate the effect of the surgical procedure in the somatosensory system [1].

The most common approach to extract relevant features from SEPs is to study the transient response to single electrical pulses. The standard procedure involves averaging the measured response over several trials (500 to 1,000) to remove background noise, and comparing the characteristics of specific components to normative data, using parameters such as peak latencies, inter-peak latencies or amplitudes [1]. In this approach, stimulus rates up to 5 Hz are commonly used [2] [1].

A more recent approach focuses on the study of the steady-state response of the brain to periodic stimulation at higher frequencies, which is denominated steady-state evoked potential. While transient evoked responses show a somewhat variable relationship between stimulus and response, steady-state evoked responses have a component that is phase-locked to the stimulation, according to their original definition [3]. Additionally, their constituent frequency components remain closely constant in amplitude and phase over a long time period [4]. It has been observed that, when stimulation is not a single event but a periodic sequence of them, the dominant frequency of the EEG corresponds with that of the stimulation [3]. Steady-state evoked potentials were recorded for the first time by Regan [3] in the visual cortex after periodic visual stimulation and have also been widely studied in the auditory modality [5] [6] [7]. More recently, studies have also investigated the steady-state response of the brain to somatosensory stimulation, using mechanical stimulation with vibration and textures [8] [9] [10], or non-nociceptive and nociceptive electrical stimulation [11] [12].

While low frequencies, usually under 5 Hz, are used for the study of the transient response to individual SEPs [2] [1], higher frequencies of stimulation are commonly used for

generation of steady-state responses. Increasing the frequency of stimulation has showed to decrease the amplitude of individual SEP components [13] [14] [15]. When the frequency of stimulation is increased and the latency and amplitude of individual SEP components are affected, it may becomes difficult to separate the rhythmic potential into segments which can be attributed to each individual stimulus in the time domain [16]. Therefore, it has been argued that, for higher stimulation frequencies, it becomes more appropriate to do analysis in the frequency domain [6].

There is a limited number of studies that have used the frequency-domain approach to study steady-state responses elicited by electrical stimulation. In studies from different sensory modalities, the recording and analysis of steady-state evoked potentials have shown several benefits when compared to the analysis of transient responses, such as a high signal-to-noise ratio (SNR) at the frequency of stimulation, shorter recordings needed in order to obtain reliable signals [17] and the possibility to frequency-tag the cortical activity elicited by different stimuli presented simultaneously [18]. Additionally, analysis of steady-state responses allows for the study of the delay and nonlinearity of sensory processing [19]. Nonlinearities in sensory processing are still not fully understood and they have potential to be clinically relevant for motor disorders [20] [21], migraine [22] and epilepsy [23] [19]. As an illustrative example of one of these benefits, Noss et al. [17] were able to obtain a reliable steady-state response from scalp electrodes overlying the somatosensory cortex in only a few seconds, while no signal was statistically discriminable from noise in the transient SEP from as much as 20 seconds of data.

Study of steady-state responses to periodic stimuli, as opposed to the traditional study of transient response to individual SEPs, enable a more in-depth study of brain responses in addition to showing several practical benefits. However, it is still not clear what characterizes this steady-state response in the somatosensory system and under which frequencies of stimulation it can be observed.

A. Motivation and contribution

In order to bridge the presented gap, this study uses time and frequency analyses with the aim of identifying measurable changes in the brain response when stimulation frequency is increased, as well as identifying a potential threshold frequency at which the steady-state appears.

1) In the time domain: As stimulation frequency increases, it is expected to observe a decrease in the detection rate and amplitude of individual SEP components. This decrease is expected to be significantly different at the threshold frequency. A significant difference in latency may also be observed.
2) In the frequency domain: It is expected to see the stimulation frequency as the predominant frequency in the EEG power spectrum. At the threshold frequency, it is expected to see a significant increase in power compared to previous frequencies.

By answering these questions, this study aims to broaden the understanding of steady-state responses in the brain and guide clinicians and researchers in the design of their experiments and the analysis of the collected data. These results could also clear the path for growing applications of periodic electrical stimulation, such as diagnosis of specific pathologies of the nervous system, modeling of cortical processing or brain-computer interfaces.

II. Methods

A. Participants

Nine healthy volunteers participated in this study. The participants were 4 men and 5 women, all right handed, and they were 23.8 $\pm$ 1.5 years old (mean $\pm$ SD). They had no previous history of neurological disorders or implanted electronic medical devices. Written informed consent was obtained from all participants. The study was approved by the Human Research Ethics committee of the Delft University of Technology (TU Delft).

B. Experimental setup

The experimental setup used for delivery of electrical stimulation and recording of EEG signals is depicted in Fig. 1.

1) Setup for electrical stimulation: Electrical stimulation was delivered transcutaneously using a battery-powered constant current stimulator (Energy stimulator, Micromed S.p.A., Italy). The stimulator was externally triggered from a laptop using a custom-made script in Matlab (The Mathworks Inc., United States). Circular stick-on TENS electrodes (diameter 3.2 cm, inter-electrode distance 3.5 cm) were placed over the median nerve at the right wrist, with the anode (positive terminal) distal to the participant. These electrodes were used as an alternative to spherical electrodes, which elicited undesired sensations of pain in pilot tests (Appendix A-B). The cables connecting the stimulator with the electrodes were shielded with a copper braided mesh that was connected to the laboratory ground, in order to reduce the magnitude of electrical artifact found in preliminary results (Appendix A-D).

2) Setup for EEG recording: Electroencephalography (EEG) was used to measure electrical activity of the brain. An electrode cap with 64 Ag/AgCl electrodes following the international 10-10 system (Infinity Gel Headcap, TMSi B.V., The Netherlands) and a 64-channel amplifier (Refa-64, TMSi B.V., The Netherlands) were used. An additional stick-on ECG electrode was used as patient ground, located behind the right ear, over the right mastoid. EEG signals and stimulation triggers were recorded using Asalab software (ANT Neuro, The Netherlands) at a sampling rate of 2,048 Hz from 62 channels (out of the 64 channels, channels M1 and M2 were disconnected).

C. Experimental procedure

1) General introduction to the experiment: Participants were welcomed into the laboratory. After explanation of the

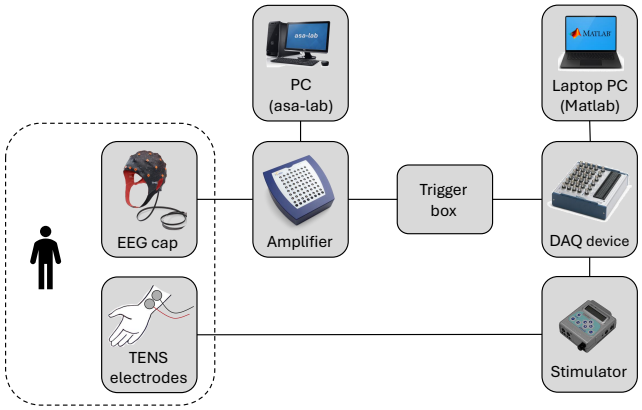

Fig. 1: Experimental setup. Participants received electrical stimulation at the median nerve through TENS electrodes on the right wrist. The stimulator was triggered using a custom Matlab script and EEG signals were recorded using Asalab software.

experiment and signing of the informed consent form, the EEG cap corresponding to their head size was fitted and gel was applied to all the electrodes until the impedance was below 10 $k\Omega$ in all of them.

2) Determination of perception threshold and familiarization with the stimulation: Introduction of the electrical stimulation to the participants was divided in two parts. First, the value corresponding to the perception threshold was determined for each participant using 500 μs rectangular pulses with a frequency of 3 Hz, increasing the amplitude is steps of 1 mA. Then, stimulation was delivered for a few seconds so that the participant would get familiar with the sensation generated by the electrical stimulation. This was done to increase comfort of the participant and reduce potential feelings of unease arising from perceiving unknown sensation.

3) Delivery of stimulation signals and data collection: In the main part of the experiment, participants were asked to sit on a chair in a comfortable position in a dim, silent room and asked to relax and fix their gaze at a specific point of their choosing. Stimulation signals were delivered and EEG data were collected.

In the past, different types of signals have been used to study somatosensory evoked potentials in the steady state, elicited by electrical stimulation of the median nerve. Some of these are pulse trains [16] [24] [25], amplitude-modulated pulse trains [11] [12], amplitude-modulated sinusoids [17] and frequency-modulated sinusoids [26]. After conducting some preliminary analyses and tests, it was concluded that even though modulated signals effectively focused the power at modulation frequencies and reduced the power at their harmonics, the high frequency of the carrier signal would make it hard to interpret response to individual pulses. Therefore, pulse trains were chosen as the most appropriate stimulation signal for this study. Preliminary analyses and test results are reported in Appendix A.

The delivered stimulation signal consisted of rectangular monophasic electrical pulses with a duration of 500 μs, and an amplitude of twice the perception threshold of each participant (the amplitude was increased 1 mA if the sensation was not clearly perceived at the threshold). Pulses were delivered in five-second trains at different frequencies: 3 Hz, 7 Hz , 13 Hz, 19 Hz and 37 Hz. These frequencies were selected because: (i) They span a wide range, (ii) they are not multiples of each other, to avoid potential misinterpretation of power observed at their harmonics, (iii) the four lower frequencies - 3 Hz, 7 Hz , 13 Hz, and 19 Hz - have a period higher than 50 ms, which is the minimum analysis time for SEPs [1] and (iv) some of them coincide with the ones used by Colon et. al [11], allowing potential comparison of some of the results.

Stimulation trains were divided in 6 blocks, with rest periods of approximately 90 s after each block. Each block was made of 22 or 23 stimulation trains, separated by intervals with a duration between 4 and 6 seconds, as represented in Fig. 2. Two of the participants didn´t receive the highest frequency, so they only received 22 stimulation trains per block. Each train had one specific frequency, and they were delivered in a pseudo-random order which was unique for each participant. Table I shows the total time of stimulation at each frequency and the total number of trains per participant. For analysis of SEPs in the time domain, a minimum of 500-1,000 pulses is often recommended [1]. In this case, a minimum of 1,000 pulses were delivered at every frequency. For analysis in the frequency domain, a reliable steady-state response has been observed from scalp electrodes overlying the somatosensory cortex in less than 20 seconds of data [17]. In this case, a minimum of 30 s of data were recorded for every frequency.

After every stimulation block, participants were asked if they could still feel the stimulation. The objective of this procedure was to make sure that the stimulation was clearly perceived by the participant throughout the experiment.

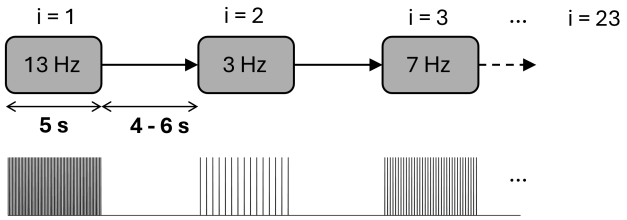

Fig. 2: Graphical representation of one stimulation block. Each block was made of 23 five-second stimulation trains, with rest periods in between them. Three trains are depicted in the figure. Pulse frequency of each train was either 3, 7, 13, 19 or 37 Hz. Each participant received 6 stimulation blocks like the one depicted in the figure, separated by rest periods of around 1.5 minutes.

TABLE I: Stimulation parameters across different pulse frequencies for each subject

Pulse frequency (Hz)	No. of 5s trains	No. of pulses
3	360	1080
7	150	1050
13	90	1170
19	60	1140
37	30	1110

D. Data analysis

1) Preprocessing: EEG data were preprocessed using EEGLAB [27], an open-source toolbox running in the Matlab environment. Three flat channels were removed, corresponding to M1 and M2 electrodes (not used) and CP3 electrode (faulty). Standard electrode spatial locations corresponding to the international 10-10 system were loaded. Noisy channels were removed following the standard EEGLAB criterion: high-frequency noise standard deviation ≤ 4 or correlation with nearby channels ≤ 0.8. Data was high-pass filtered using the finite impulse response (FIR) filter from EEGLAB, using a cutoff frequency of 1 Hz in order to remove slow drifts in the data.

2) Time domain analysis: Data was further processed using Matlab and EEGLAB. Potential stimulation artifact was eliminated by interpolating data from the onset of each pulse to 8 ms after the onset of each pulse and adding normally distributed random noise. This modification only affected visualizations in this time range and not numerical analyses, as data in this time range was not analyzed. Continuous EEG data were low-pass filtered using the default finite impulse response (FIR) filter from EEGLAB, with a cutoff frequency of 250 Hz. Cortical SEP components are normally observed in the signal from electrodes overlying the somatosensory cortex, contralateral to the side of stimulation [1]. Epochs were extracted from electrode C3 time-locked to every stimulation pulse, starting 10 ms before each pulse and ending 300 ms after each pulse, and divided in subsets corresponding to each stimulation frequency. For a visual evaluation of the results, single trials as well as the average across epochs were plotted using the "ERP image" function from EEGLAB.

In order to further analyze the data, amplitudes and latencies of four characteristic SEP components (positive and negative peaks in the average response) were extracted. With this purpose, continuous data was further low-pass filtered with a cutoff frequency of 100 Hz in order to reduce high-frequency oscillations which were not relevant for this specific analysis. Once again, epochs were extracted from electrode C3 around every stimulation pulse, starting 10 ms before each pulse and ending 50 ms after each pulse. Data was divided in five subsets corresponding to each stimulation frequency and averaged across epochs in each of them. Specific latencies for SEP components may vary per subject depending on factors such as height and arm length [28]. Using a custom Matlab function, local minima were found for each subject and stimulation frequency around latencies 20 ms and 35 ms after every stimulation pulse, and local maxima were found around latencies 25 ms and 40 ms after every stimulation pulse. These extrema were labeled as components N20, N35, P25 and P40 respectively, where the number refers to their nominal latency, which is not necessarily the exact latency due to different factors such as the mentioned between-subject variability or the frequency of stimulation, which is investigated in this study. In this report, these components are also referred to as components 1, 2, 3 and 4, in increasing order of latency. Single-subject data was evaluated visually for the presence of SEPs and the detection of the four components. Additionally, the scalp topography at the latency of the P40 component was extracted for every subject and averaged across subjects for every stimulation frequency separately. Only channels that were present in all subjects (i.e. not removed during preprocessing) were used for the grand average.

Even though characteristic SEPs components may vary in amplitude and latency per subject, an average across subjects can still provide an overall perspective of the behavior of the cortical response [29]. In order to obtain a global visual confirmation of the presence of SEPs, epochs were averaged across subjects separately for every stimulation frequency.

Furthermore, statistical analyses were conducted for evaluating the effect of the frequency of stimulation on the amplitude and latency of each SEP component using IBM SPSS Statistics (Version 29.0). The features amplitude and latency were evaluated with individual tests for each SEP component (each peak). For each feature and each peak, Saphiro-Wilk tests were used to evaluate normality of the data in each sample. Afterwards, Friedman tests (8 in total) were conducted in order to identify differences in latency or amplitude among frequencies of stimulation. When a significant difference was found, post-hoc pairwise comparison tests were used to find which pairs were significantly different.

3) Frequency domain analysis: True frequency of stimulation may sometimes be different to the nominal frequency due to timing inaccuracies in the hardware to generate the stimulus [30]. Before conducting any analysis in the frequency domain, it was important to know the true frequency at which stimulation was being delivered. Event data recorded simultaneous to the EEG data were used to calculate the true instantaneous frequency of stimulation for every stimulation train of every subject. These values were averaged across trains of all subjects with the same nominal frequency, and the resulting values were rounded to the nearest integer and used for further calculations instead of the nominal frequencies.

Channels that presented large values of artifact were removed. With this purpose, epochs were extracted time-locked to every stimulation pulse starting 11 ms before every pulse and ending 11 ms after every pulse. Data were averaged across all epochs (>4,000 epochs) for each subject. Channels that, when averaged across all epochs for each subject, presented values that were higher than three scaled median absolute

deviations from the median of all channels (outliers) in the analyzed time range were removed.

In Matlab, continuous EEG data were low-pass filtered using the finite impulse response (FIR) filter from EEGLAB, with a cutoff frequency of 250 Hz. Stimulation epochs with a duration of 5 seconds were extracted from the data of each subject, starting at the beginning of each stimulation train. Data were grouped in five datasets, each dataset containing data corresponding to one stimulation frequency, which were analyzed separately. For each channel and each epoch, the power spectral density (PSD) was calculated using the Welch method using a Hamming window with a length of 1 second (number of samples equal to the sampling rate of 2,048 Hz) to get a resolution of 1 Hz, and no overlap between windows. The obtained power spectra were then averaged across epochs and across subjects for each dataset. The average and standard deviation of the PSD at electrode C3 was plotted for each stimulation frequency. In order to investigate the relative distribution of power across the scalp, power at the frequency of stimulation was extracted for each dataset, averaged across subjects and plotted as a scalp topography.

Signal power at the stimulation frequencies is expected to correspond to the sum of the stimulus-evoked response and background noise. To obtain a measurement that represents the stimulus-evoked response, the SNR was calculated for each dataset at the corresponding stimulation frequency by subtracting, from the power at the stimulation frequency, the mean power at the two adjacent frequencies (± 1 Hz) [12]. It must be noted that, strictly speaking, this value represents a difference rather than a ratio and therefore it carries units. Additionally, to evaluate whether this SNR was different from zero, Wilcoxon signed-rank tests were used, after normality of the data was rejected by Shaphiro-Wilk tests. For the conditions (i.e. stimulation frequencies) that were significantly different from zero, an additional Wilcoxon signed-rank test was used to test the difference in SNR between them.

4) Artifact analysis: Efforts were made to reduce electrical artifact as much as possible with the experimental setup, as described in Section II-B. However, as experienced by other researchers [31], it is common that some artifact caused by electrical stimulation will remain in the data. In order to investigate the presence of this artifact, epochs were extracted time-locked to every stimulation pulse starting 11 ms before every pulse and ending 11 ms after every pulse. Data were averaged across all epochs (>4,000 epochs) for each subject. Data was analyzed visually for every subject separately. Magnitude of the artifact was extracted for every subject and channel.

Before analysis in the frequency domain, removal of artifact was attempted by simple methods including interpolation with some variations and plain removal of artifactual samples. Detailed information about these attempts is reported in Appendix B. After evaluation of the effect of these methods on the frequency spectra, none of them was adopted. As an alternative, channels that showed high magnitude of the artifact were removed as described in Section II-D3.

A post-hoc artifact analysis was conducted to estimate the effect of the artifact on the frequency spectrum of channel C3. After removal of channels that showed high magnitude of the artifact as described above, EEG data were re-referenced to a common average for each subject in order to reduce the amplitude of the artifact. Then, the frequency spectra and the SNR at the frequency of stimulation were compared to the values obtained before re-referencing.

III. Results

A. Perception threshold and amplitude of stimulation

The mean perception threshold across all subjects was 2.56 mA, and the mean amplitude of stimulation was 5.3 mA. Specific values for perception threshold and amplitude of stimulation for each subject are presented in Table II. The amplitude of the stimulation used for the experiment was twice the perception threshold of each participant. The amplitude was increased 1 mA if the sensation was not clearly perceived at the threshold. This was the case for two of the participants. The amplitude was maintained at the same value throughout the experiment for each participant. All participants reported to perceive the stimulation after every stimulation block until the end of the experiment. One participant reported to feel pain after the first stimulation block. At this point, the amplitude was reduced by 1 mA, and the sensation of pain receded.

TABLE II: Perception threshold and stimulation amplitude for each subject

Subject ID	Perception threshold (mA)	Amplitude of stimulation (mA)
1	6	12
2	1	2
3	2	4
4	3	6
5	2	5
6	2	4
7	2	5
8	3	6
9	2	4

B. Time domain analysis

SEP data was initially evaluated visually at a single-subject level. Similar observations were made for all subjects, except for subject 4, which presented faulty data and was therefore excluded from any further analysis. As an illustrative example, Fig. 3 shows data corresponding to one single subject (subject 6), extracted around every stimulation pulse, and divided by stimulation frequency. The first column shows the amplitude across time for >1,000 epochs. Single trials are displayed as a heatmap, aligned by the latency with respect to the onset of the pulse. The blue line at the bottom represents the average across all the epochs above. An ”M” shape, starting around 20 ms, can be observed at every stimulation frequency. Visually, it becomes apparent that the shape presents variations when the frequency increases. For the lowest frequency (3 Hz), the period between subsequent pulses is above 300 ms. Therefore, we observe one single visible response in the 300 ms window.

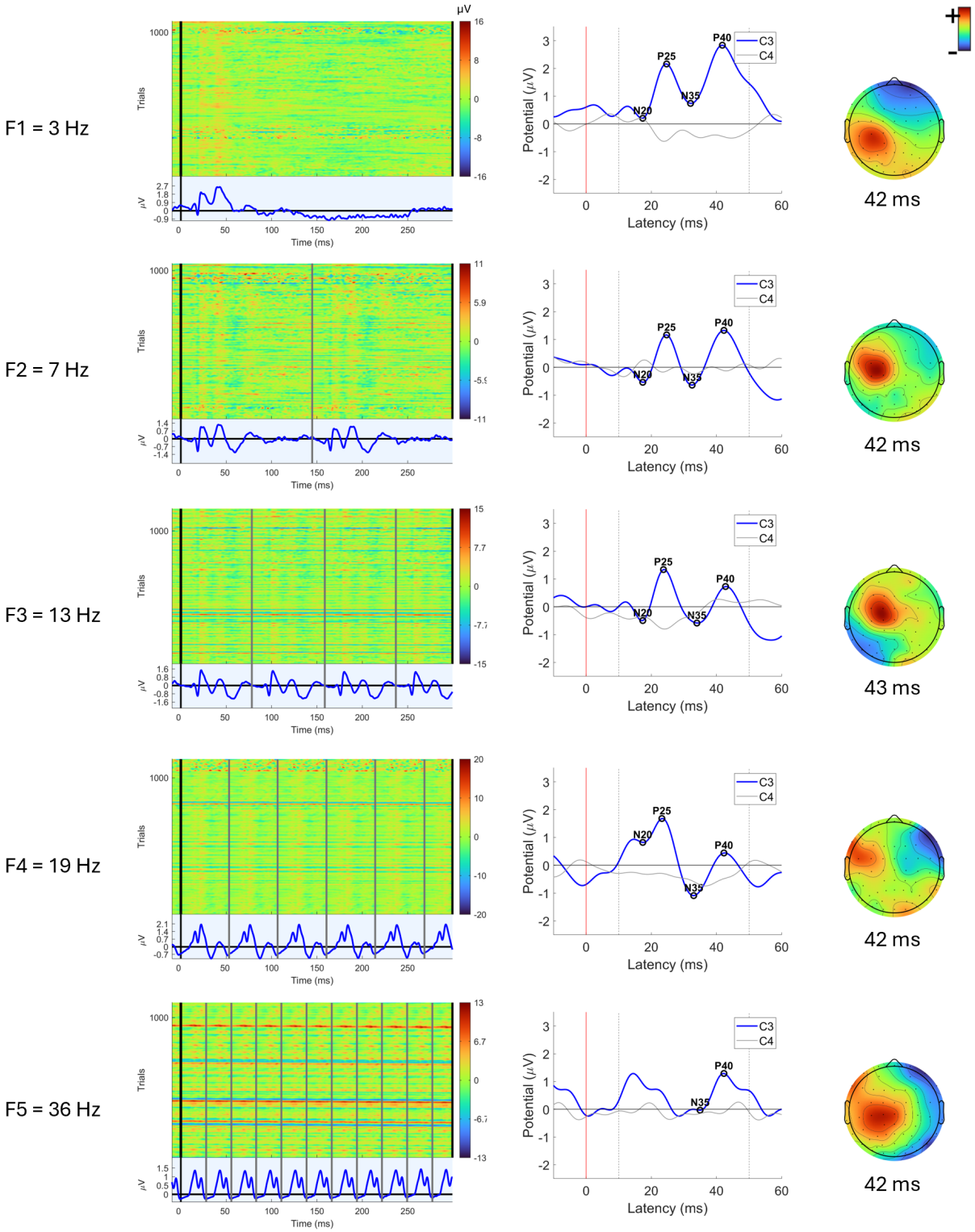

Fig. 3: Illustrative example of data from one subject (subject 6). Each row of subfigures corresponds to one stimulation frequency (F1 to F5). The first column shows electric potential (μV) recorded at electrode C3 along time, averaged across multiple epochs (>1,000). Here, single trials are displayed as a heatmap and the blue line at the bottom represents the average. The second column displays the results of the component detection, where components N20, P25, N35 and P40 can be observed, in this order in time. The third column shows the relative potentials across the scalp at the latency of component P40.

Afterwards, the potential decreases and stays around zero. For the next frequency (7 Hz) the period is 143 ms. Therefore, we can observe the response to two pulses in the 300 ms window. We can still observe that the potential returns to values around zero after the oscillations. For the next frequency (13 Hz), the period of 77 ms allows to see four SEP responses in the 300 ms window. In this case, the potential does not return to values around zero, and it shows one SEP response after another. This is also the case for the next two frequencies (19 Hz and 36 Hz), where SEP responses are consecutive.

The second column of Fig. 3 shows the results of the component detection for the same subject. In this specific subject, four components were detected around the expected latencies for all frequencies except the highest one (F5), and they were labeled as the four characteristic SEP components. Table III presents a summary of the amplitudes for all components in all subjects, where cells are shaded in gray if one or more components were not detected. It can be seen that, out of the 8 subjects, the four components were detected in 7 subjects for F1 (3 Hz), in 6 subjects for F2 (7 Hz), in 5 subjects for F3 (13 Hz), in 7 subjects for F4 (19 Hz) and in only 1 out of 6 subjects for F5 (37 Hz).

The third column of Fig. 3 shows the relative scalp topography at the latency of P40 and the numerical value of this latency. These single-subject heatmaps of relative potential across electrodes show lateralization with higher activation on the left side of the scalp. Individual SEP waveforms and detected components for every subject can be found in Appendix C.

The grand average of the SEP (across subjects), displayed in Fig. 4 is a visual summary of the activity recorded by electrode C3 at every stimulation frequency. Local extrema can be visually identified (blue bars). For components N20, P25 and P4, all the frequencies generated a grand-average component around the expected latencies. For component N35, all frequencies except for the highest one (F5, green line) generated a local minimum around the expected latency.

Scalp topographies were extracted for each subject at the latency of component P40 in electrode C3 and then averaged across subjects. Average topographies for each stimulation frequency are displayed in Fig. 5, showing the relative amplitude of all scalp electrodes at the latency of this component. All topographies show the highest potential at the side contralateral to the stimulation. Topographies for F2 and F3 show clear maxima centered at the left central electrode C3 and a potential that decreases gradually across the scalp, with weak negativities on the right hemisphere. Distributions for F1 and F3 show similarities, where there is a clear maximum in the centro-parietal region over the left somatosensory cortex, on the area above electrodes C3, C5, CP3 and CP5. These topographies show a strong polarity inversion, with negative values contralateral in the scalp, in the right frontal region. The topography at F5 shows a strong left central positivity that attenuates toward the right hemisphere, with a minor contralateral negativity over the right posterior region. Regarding relative amplitude, F1, F2, F3 and F5 show strong maxima, and F4 shows a slightly weaker and more disperse maximum.

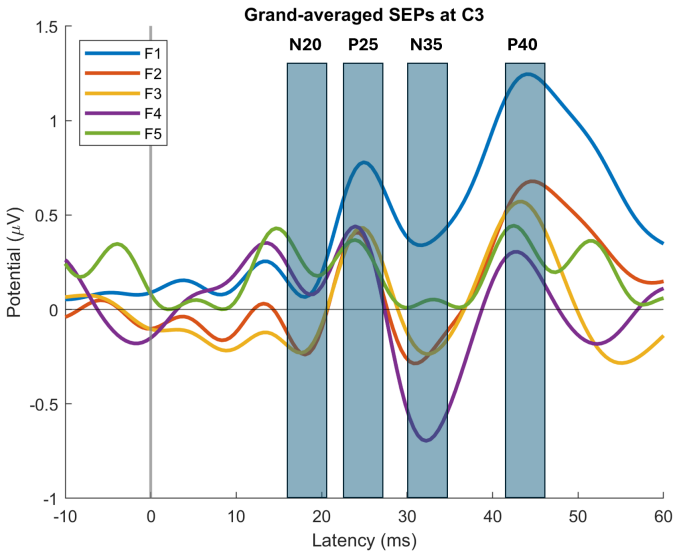

Fig. 4: Somatosensory-evoked potential (SEP) average across all subjects, for each stimulation frequency (F1 to F5). Ranges for the locations of SEP components N20, P25, N35 and P40 are highlighted. Specific component latencies may vary per subject. Therefore, this grand average was used solely for illustration purposes.

Amplitude of each of the four components in the SEP (N20, P25, N35 and P40) were compared between frequencies of stimulation. These data are displayed in Fig. 6. Components 2, 3 and 4 show an overall trend in which the amplitude decreases from frequencies F1 to F4, to then increase again or stay constant at F5. In component 1, the amplitude decreases from F1 to F3 to then increase in F4. The largest differences between frequencies are observed in component 4, where the median value of the amplitude decreases a 77% from F1 to F4 and a 79% from F1 to F5.

Repeated measures statistical tests were used to evaluate the effect of stimulation frequency on amplitude of each component. After normality in the data was rejected for some of the groups as concluded from Shapiro-Wilk tests (Appendix D-A), Friedman tests were selected. A significant difference in amplitude was found between the different stimulation frequencies for component 3 ($\chi^2(3) = 10.1$, $p = 0.04$) and component 4 ($\chi^2(3) = 17.8$, $p = 0.001$). For component 1 and component 2 no significant differences were found (both $\chi^2(3) \leq 5$, $p \geq 0.17$). Post-hoc pairwise comparison tests, after Bonferroni correction for multiple comparisons, failed to detect a statistical difference for any specific pair in component 3. In component 4, a statistically significant difference in amplitude was found between F1 and F4 ($T = 3.8$, $p = 0.001$) and between F1 and F5 ($T = 3$, $p = 0.03$). More details about the statistical analysis are reported in Appendix D-A.

Additionally to amplitudes of the components, latencies were also investigated. Latency of each of the four components in the SEP (N20, P25, N35 and P40) were compared between

TABLE III: SEP amplitudes (μV) for every subject, frequency (F1-F5), and component (C1-C4). Gray cells indicate that not all components were detected for that subject and frequency. A dash (–) in white background indicates that data was not collected. Excluding F4, the number of gray cells increases with frequency, starting with only 1 cell for F1 and increasing up to 5 cells in F5. Data from subject 4 is missing because it was found to be faulty and was excluded from all analyses.

Subject	F1				F2				F3				F4				F5			
	C1	C2	C3	C4	C1	C2	C3	C4	C1	C2	C3	C4	C1	C2	C3	C4	C1	C2	C3	C4
1	0.11	0.43	0.26	2.09	-0.07	0.21	-0.19	1.49	0.06	0.37	-0.11	0.93	-0.14	0.07	-0.66	0.53	–	–	–	–
2	-0.09	0.48	-0.16	0.94	–	–	-0.37	0.59	–	0.32	-0.36	0.33	-0.06	0.07	-0.49	0.08	–	–	–	–
3	-0.09	0.01	-0.14	1.16	-0.53	-0.21	-0.28	0.86	-0.27	0.09	-0.26	0.52	0.13	0.19	-0.78	0.19	–	–	-0.01	0.35
5	–	–	0.98	1.53	-0.24	–	0.49	0.96	–	0.25	0.13	0.42	-0.46	-0.45	-0.74	0.17	-0.56	–	–	0.27
6	0.14	2.08	0.71	2.73	-0.55	1.21	-0.59	1.33	-0.55	1.34	-0.61	0.68	0.87	1.73	-1.01	0.45	–	–	-0.16	1.20
7	-0.70	0.86	-1.54	1.55	-0.20	1.05	-1.23	0.99	-0.97	-0.04	-1.27	1.27	-0.01	0.59	-1.40	-0.16	-0.27	0.28	0.03	0.16
8	-0.77	0.76	-1.16	3.76	-0.87	0.26	-1.91	1.19	-1.03	0.60	-2.24	–	-0.08	1.32	-2.20	–	0.34	–	-0.35	1.36
9	0.22	1.16	0.20	1.40	0.18	0.94	-0.04	1.16	0.12	0.83	-0.23	0.69	-0.03	0.42	-0.44	0.58	–	–	-0.25	0.34

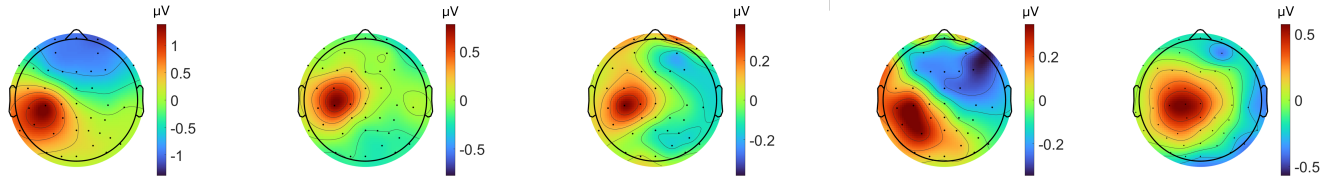

(a) F1 = 3 Hz (b) F2 = 7 Hz (c) F3 = 13 Hz (d) F4 = 19 Hz (e) F5 = 36 Hz

Fig. 5: Relative electric potential (μV) across the scalp at the latency of component P40, averaged across all subjects. Specific latency for component P40, and topography at this latency, was extracted for every subject and frequency. Topographies were averaged across subjects. Only electrodes present in all subjects were included in the average. Subfigures a-e show the result obtained from each stimulation frequency.

frequencies of stimulation. These data are displayed in Fig. 7. No obvious trends were observed in all the components as frequency of stimulation increased. It could be inferred from the figure that the variation in the data within each group is often larger than the difference between the groups, making interpretation difficult. As some observations, for components 1 and 3, the median latency at F5 is higher than for the rest of the frequencies. For component 2, the median latency is lower at F4 than for the rest of the frequencies. No further results could be extracted from visual evaluation of the data.

The same statistical analyses used for amplitude data were also used for latency data. Normality in the data was rejected for some of the groups as concluded by Shapiro-Wilk tests (Appendix D-B). Friedman tests concluded that there were no statistically significant differences in component 1, component 3 or component 4 (all $\chi^2 \leq 4.7$, $p \geq 0.3$). A statistically significant difference in latency was found between the different stimulation frequencies for component 2 ($\chi^2(3) = 10.7$, $p = 0.01$). Post-hoc pairwise comparison tests, after Bonferroni correction for multiple comparisons, failed to detect a statistical difference in latency for any specific pair in component 2. More details about the statistical analysis are reported in Appendix D-B.

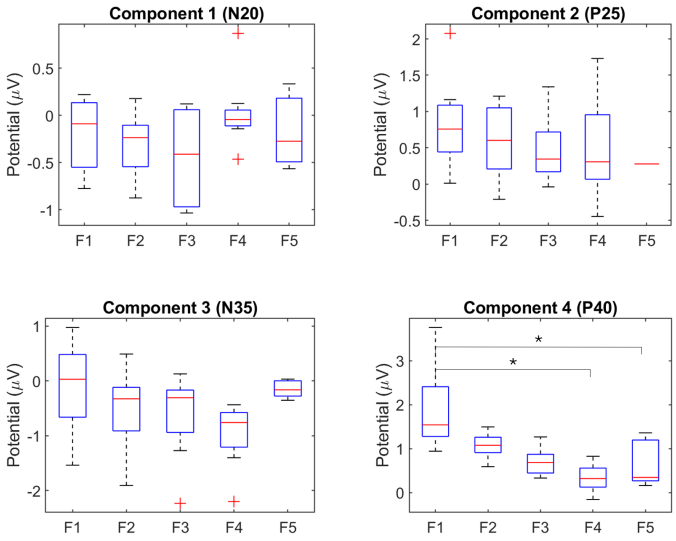

Fig. 6: Comparison of the amplitude of each SEP component across stimulation frequencies. The only pairwise significant differences, marked with an asterisk (*), were found in component 4, between F1-F4 and between F1-F5. An overall trend was observed in components 2, 3 and 4 in which the amplitude decreases from frequencies F1 to F4, to then increase again or stay constant at F5.

C. *Frequency domain analysis*

Before conducting any analysis in the frequency domain, it was important to know the true frequency at which stimulation was being delivered, which may have been different from the

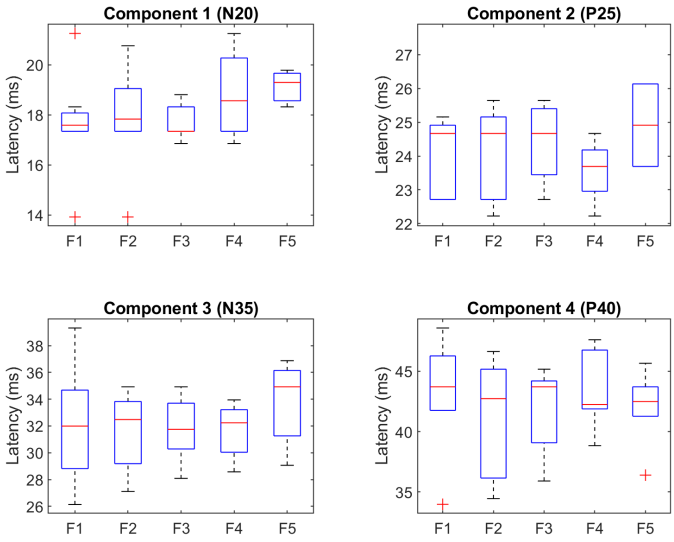

Fig. 7: Comparison of the latency of each SEP component across stimulation frequencies. No pairwise significant differences were found. No obvious trends were observed in latency of all the components as frequency of stimulation increased. The figure shows that variation in the data within each group is often larger than the difference between group medians.

nominal frequency due to hardware inaccuracies [30]. True instantaneous frequencies of stimulation were calculated from stimulation event data recorded simultaneous to the EEG and averaged across subjects for every stimulation frequency. Results are displayed in Table IV. The highest nominal frequency, 37 Hz, was found to have an average instantaneous value of 36.15±0.69 Hz. Therefore, the rounded value of 36 Hz was used for further analysis instead of 37 Hz. The rest of the frequencies, when rounded to the nearest integer, presented a true value equal to their nominal value.

TABLE IV: True instantaneous frequencies calculated from stimulation event data recorded simultaneous to the EEG.

Nominal frequency (Hz)	True frequency (Hz, mean ± SD)
3	2.93
7	6.85
13	12.64
19	18.51 ± 0.12
37	36.15 ± 0.69

The PSD of data from channel C3 was calculated for every stimulation frequency separately. These results are displayed in Fig. 8a-e (average and standard deviation). For all stimulation frequencies, the power showed high values for frequencies below 4 Hz, and also at frequencies in the alpha band (8-12 Hz). By visual inspection of the graphs corresponding to the PSD of the higher frequencies (F4 and F5), it became apparent that there was an increase in power at the stimulation frequency compared to the surrounding frequencies. This peak is marked with a black arrowhead in Figs. 8d and 8e. However, for the lower stimulation frequencies (F1, F2 and F3), no such a peak was found by visual inspection.

SNR was calculated as a measure of the stimulus-evoked response, excluding background activity non-related to the stimulation. The results across subjects (N=8 for F1 to F4 and N=6 for F5) are displayed in Fig. 8f. An increasing trend in SNR was found when the stimulation frequency was increased. From looking at the figure, it can be seen that the median SNR increases for every frequency as compared to the previous one. It also becomes apparent that the median value for the SNR is below zero for F1 to F3 and above zero for F4 and F5. The SNR at the stimulation frequency was statistically tested against zero for each of the datasets. Wilcoxon signed-rank tests concluded that the SNR was not different from zero for frequencies F1, F2 and F3 (all $W \geq 7$, $p \geq 0.12$). The SNR at the stimulation frequency was found to be statistically different from zero for the higher frequencies F4 ($W = 26$, $p = 0.043$) and F5 ($W = 21$, $p = 0.028$). An additional Wilcoxon signed rank test concluded that the SNR was not statistically different between F4 and F5 ($W = 19$, $p = 0.075$). More detailed information about these statistical analyses is reported in Appendix D-C.

The relative distribution of power across the scalp at the stimulation frequencies is displayed in Fig. 9. Overall, central regions showed relatively low power (dark blue) compared to frontal, occipital or lateral regions. As the frequency increased, these areas of low power were observed to shift from frontal to parietal regions, and also from bilateral to unilateral scalp distributions. At the lowest frequency, 3 Hz, there was a bilateral decrease in power in the fronto-central region, while the highest power was found to be located in the frontal region of the scalp. For the next stimulation frequency, 7 Hz, a similar topography was found, with the regions of low power slightly more distal and more central. For the next frequency, 13 Hz, the region of low power was located over midline central and centro-parietal electrodes, with regions of higher power located in the occipital region. For the stimulation frequency of 19 Hz, the region of low power was located on the right central and centro-parietal regions, and the topography showed a clear lateralization in which the power was higher at the side contralateral to the stimulation. For the highest stimulation frequency, 36 Hz, there was again a clear lateralization in which the power was higher at the side contralateral to the stimulation. The region with the lowest power shifted towards the back when compared to the previous frequency, now being located in right centro-parietal and parietal regions.

D. Artifact analysis

Visualizations of the data showed presence of electrical artifact in every subject. Artifact in one individual subject is presented in Fig. 10a as an illustration. The artifact was observable as peaks in the data with either positive, negative or both polarities at latencies from 0 to 6 ms after every stimulation pulse, and with maximum magnitudes which varied across subjects. When averaged across epochs, the lowest maximum value across all channels was below 1.5 μV and the highest maximum was above 40 μV. Channels where the magnitude

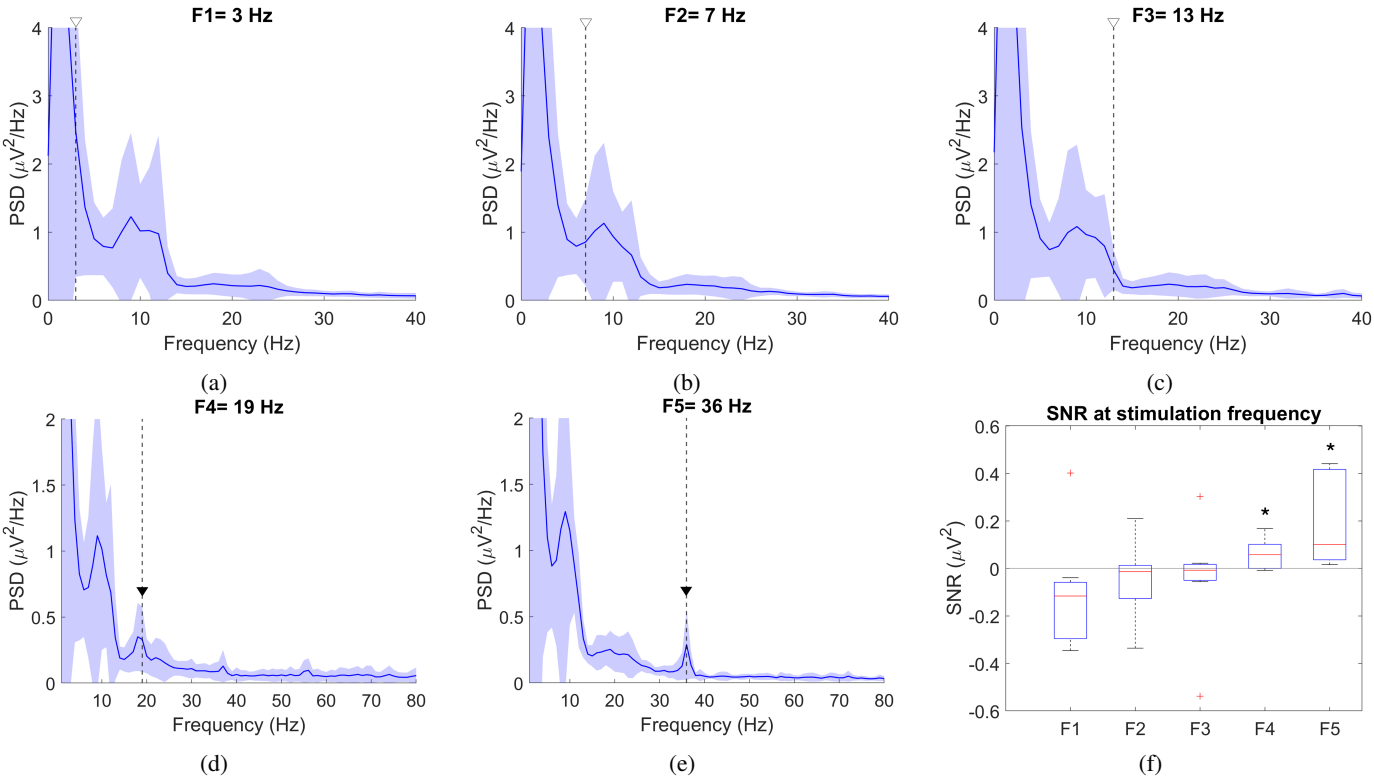

Fig. 8: (a-e) Power spectral density of channel C3 for every stimulation frequency, averaged across subjects. The solid blue line represents the average and the shade represents the standard deviation. Vertical dashed lines with arrow heads indicate the stimulation frequency. (f) Comparison of SNR at the frequency of interest for each stimulation frequency. SNR was calculated for each dataset at the corresponding stimulation frequency by subtracting, from the power at the stimulation frequency, the mean power at the two adjacent frequencies (±1 Hz) An outlier in F1 with value -2.3455 μV was left outside of the plot limits to improve the scale for visualization.

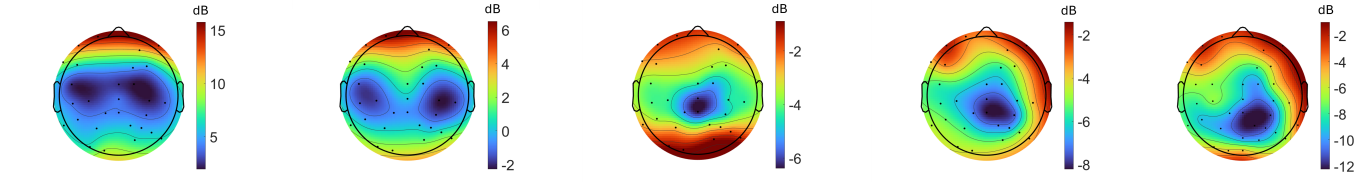

(a) F1 = 3 Hz (b) F2 = 7 Hz (c) F3 = 13 Hz (d) F4 = 19 Hz (e) F5 = 36 Hz

Fig. 9: Relative power (dB) across the scalp at the frequency of interest, averaged across all subjects. Power at the frequency of interest was extracted from the PSD for every channel and subject and it was averaged across subjects. Only electrodes present in all subjects were included in the average.

of the artifact was an outlier compared to all channels in that subject were removed. After removing outliers, the artifact was present to some extent across all the scalp in all subjects, as illustrated in Fig. 10b with data from one subject. Regarding location, no specific repeatable pattern was observed across subjects. Figures for all subjects are reported in Appendix E.

In the post-hoc artifact analysis, the magnitude of the artifact was reduced for 7 out of the 8 subjects when re-referencing the data to a common average (reduction of 48 ± 25% across the 7 subjects). The SNR at the stimulation frequency showed a smaller decrease (reduction of 17 ± 10% across 6 subjects, excluding an outlier where the reduction was 688%). Additional figures displaying these results are reported in Appendix E.

IV. Discussion

The objective of this study was to investigate the effect of stimulation frequency on the response of the somatosensory cortex to electrical stimulation, and to evaluate whether a transition to the steady-state could be found in the cortical SEP at a specific stimulation frequency. This transition was expected to be marked by a significant decrease in component

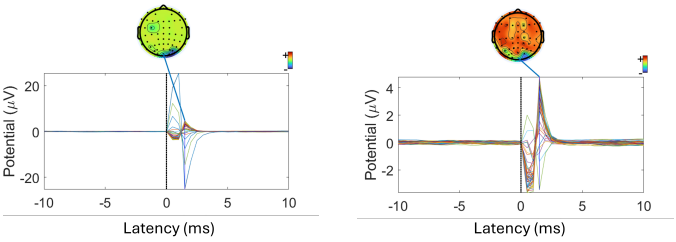

(a) Original (all channels) (b) After removing 5 channels

Fig. 10: Electrical artifact for one of the subjects (subject 1), before and after removing the channels with highest amplitude. Average across >4,000 epochs time-locked to every stimulation pulse, and topography at the time of maximum amplitude. Each line is one channel. Latency 0 corresponds to the time of delivery of the electrical stimulation. Notice that the value of the y axis is different for both subplots.

amplitude in the time domain and a significant increase in power at the stimulated frequency, detectable by analysis in the frequency domain.

A. Observations in the time domain

In the time domain, SEPs showed an "M" shape formed by components N20, P25, N35 and P40, characteristic of somatosensory responses after stimulation in the upper limb [32]. Observations from single subjects, which showed characteristic wave shapes and topographies, indicated that SEPs were being elicited by the stimulation and that the signal recorded at electrode C3 could be used as a representation of the somatosensory response. The quantitative evaluation of the presence of this "M" pattern at a group level was conducted through the detection of the components in every subject. Not all the components were detected in all subjects for all frequencies. As expected, all four components were found in most subjects at the lowest stimulation frequency (7 out of 8 subjects). For the rest of the frequencies, the number of subjects at which the four components were detected decreased sequentially for the frequencies of 3 Hz, 7 Hz, 13 Hz, and 36 Hz, with the four components only being detected for one of the subjects at the highest stimulation frequency. Early components were often the ones missing, while late components remained detectable. This observation is in accordance with the expected transition of the response from a complex waveform (the characteristic SEP shape) to a simple sinusoid when frequency is increased. It must be noted that the 19 Hz frequency was outside of this trend, as the four components were detected for most subjects (7 out of 8) at this stimulation frequency. We could identify individual components for most subjects in frequencies up to 19 Hz, even though amplitudes were relatively low for some of them. Some studies reported peaks not being detectable after individual stimuli for most subjects at a frequency of 10 Hz [14] [15] while others have reported being able to increase the stimulation frequency up to 8 Hz without significant loss in the detectability of most components [33]. Differences in experimental design could explain the fact that we could identify the components for frequencies higher than previously reported. As some examples in these differences, Pratt et al. [33] conducted very long recording sessions of 4-5 hours, during which subjects usually fell asleep, while our recording sessions were always under 1 h. Delberghe et al. [13] used cup electrodes while we used TENS electrodes, and García-Larrea et al. [15] used pulses with a duration of 0.2 ms, while our pulses were 0.5 ms long. An effect of the duration of the experiment on the results is expected due to factors like drowsiness of the subject and habituation to the stimulation. The effect of the choice of electrodes or the duration of the pulse on the results is an effect that we experienced during pilot tests. Differences in electrode shape and pulse width have an influence on the current that is delivered to the median nerve. The measured SEP is a sum of the contributions from different fibers that respond to the stimulus. As the current is increased, additional fibers are recruited, and recruitment of smaller diameter fibers is reflected in the SEP with the appearance of additional components [31]. This phenomenon is normally observed in peripheral recordings, but could also have an influence on cortical recordings. All these factors indicate that choices during experimental design are influential on the results, which increases the complexity of between-study comparisons.

A significant difference was found in the amplitude of components P25 and P40 between frequencies. For component P25, even though this significance was not attributed to a specific pair of frequencies by pairwise post-hoc tests, an overall trend could be observed in which the amplitude of the P25 component consistently decreased when stimulation frequency increased from 3 Hz to 19 Hz. The same decrease in amplitude was observed for P40 when stimulation frequency increased. In the case of P40, this difference was significant between the amplitude at 3 Hz and 19 Hz, and also between the amplitude at 3 Hz and 36 Hz. This decrease in amplitude was expected, as previous studies have also found a reduction in the amplitude of some SEP components when increasing stimulation frequency [13]. Most of these studies only explored frequencies up to 10 Hz, finding a significant decrease in frontal N30 when changing stimulus frequency from 2 Hz to 5 and 10 Hz [14] [29].

For components N20 and N35, we found no significant differences in amplitude between stimulation frequencies. It is a common observation that the amplitude of some components is affected by stimulation frequency while the amplitude of other components is not, and it could indicate that the compared components are generated by separate neural structures [13].

Latencies of the SEP components did not change significantly across stimulation frequencies in this study. A few studies reported similar results, with minor and not statistically relevant latency changes in several components when increasing stimulation frequency up to 10 Hz [14] [15].

Scalp topographies at the latency of the P40 component, averaged across subjects, consistently showed activation centered around the contralateral side to the stimulation, as expected.

Several lines of evidence strongly support the conclusion that cortical SEPs in the 20-40 ms latency range are generated in contralateral somatosensory cortex in areas 3b and 1 [34]. Topographies for stimulation at 3 Hz and 19 Hz showed maxima over parietal regions as previously observed in several studies [16] [12] and as expected due to the location of the somatosensory cortex.

When looking at the topographies for the frequencies of 7 Hz, 13 Hz, and 36 Hz, it could seem like the response was focused above the central sulcus rather than behind it, as central electrode C3 showed a compact maximum rather than the maximum being spread towards centro-parietal electrodes. A potential explanation for this topography could be that the motor cortex, located just anterior to the central sulcus, was also activated simultaneously to the somatosensory cortex during our experiments. This would be a plausible explanation given that the stimulus intensity commonly used to elicit the SEPs activates predominantly the large diameter fast conducting sensory fibers, including group IA muscle afferents and group II cutaneous afferents, and there is some controversy as to the relative proportion of muscle and cutaneous afferents contributing to the cortical response [35] [36]. However, an alternative and more simple explanation could be that the C3 electrode was actually located above the postcentral gyrus during data collection, as analyses of craniocerebral topography have found that electrodes C3 and C4 may overlie either the postcentral or precentral gyri, depending on individual anatomy [37] [38]. Assuming that this was the case, our results would be in accordance with previous findings.

The clear polarity reversal observed for the frequencies of 3 Hz and 19 Hz has also been reported by previous studies, and it has been related to a tangential source of activity originating from the primary somatosensory cortex (S1). Our results showed disappearance of the negative frontal field when increasing the frequency from 3 Hz to 7 Hz. Garcia-Larrea et al. [15] also reported the disappearance of a negative frontal field (in their case related to component N30) when increasing the stimulation frequency from 2 to 10 Hz, but they did not provide a hypothesized reason. A potential explanation would be that, when increasing stimulation frequency, the total response results from a complex superposition of response components from different cortical sources, which can obscure the inversion of polarity [39]. However, more evidence would be necessary to support this hypothesis, and this would still not provide a reason why this polarity reversal appears again at the frequency of 19 Hz, which remains unknown.

B. Observations in the frequency domain

Characteristic SEP waveforms and topographies were observed in the time domain for every stimulation frequency. Therefore, we also expected to observe peaks in the frequency spectra for every stimulation frequency. For the stimulation frequencies of 19 Hz and 36 Hz, clear peaks were observed in the spectra, indicating that those frequencies predominated in the EEG over adjacent frequencies. In other words, the stimulus-evoked response at the stimulation frequency was higher than the background brain activity, non-specific to the stimulation. These peaks were accompanied by an SNR significantly different from zero (calculated as the difference between the power at the stimulated frequency and the power at adjacent frequencies). For the lower frequencies of stimulation (3 Hz, 7 Hz, and 13 Hz), salient peaks were not found in the frequency spectra, and the SNR was statistically not different from zero.

Some results from previous studies support our findings. Namerow et al. [16] used two scalp needle electrodes to explore stimulation frequencies from 12 to 200 Hz and found an apparent transition in the nature of the response between the frequencies of 20 Hz and 40 Hz. They used narrow-band filters centered at the frequency of stimulation to explore the responses. At frequencies of 40 Hz and above, the response at the frequency of stimulation showed a relatively constant amplitude and phase, resembling a simple sinusoid.

Steady-state SEPs are often considered to originate from an entrainment of neurons responding to the periodic somatosensory stimulation [8] [4]. At some stimulation frequencies, a resonance-like phenomenon is thought to occur, which has been related to the temporal characteristics of the neurons constituting the resonating network [40]. Following this hypothesis, specific frequencies have been found in the auditory and visual modalities that show clearly salient peaks in the frequency spectrum. In the somatosensory modality, studies that used vibratory stimulation also found these resonance-like frequencies, which have been located by different researchers around 21 Hz [10], 26 Hz [41], and 27 Hz [8].

In the case of transcutaneous electrical stimulation elicited by pulse trains, this entrainment seems to appear at frequencies of 19 Hz and above, according to our results. Su et al. [42] compared the responses to 20 Hz and 40 Hz stimulation with frequency domain analysis and observed a significant increase in amplitude at the frequency of stimulation when increasing the stimulation frequency. We also observed a higher response to the 36 Hz stimulation when compared to 19 Hz, but in our case, the difference was not statistically significant. Because we only observed this salient spectral peaks at the frequencies of 19 Hz and 36 Hz, it is hard to assess whether any resonance-like phenomenon occurred.

Two recent studies from the same research group used transcutaneous electrical stimulation, similar to the one used in our study, as a control for their experiments about nociceptive stimulation [11] [12], and they reported finding salient peaks in the frequency spectra for different frequencies in the range 3 to 43 Hz. We expected to see similar peaks for all of our stimulation frequencies. However, this was not the case for the frequencies of 3, 7 and 13 Hz. The stimulation signals used in these studies were different from ours, which could be the reason for the different results. These studies used pulse trains with carrier frequencies above 180 Hz, modulated by a repeating boxcar function. Therefore, what they referred to as "stimulation frequencies" were actually the modulation frequencies of a higher-frequency carrier signal. Potentially, the modulated signal with a high-frequency carrier elicited

the neuronal entrainment that led to observable peaks in the spectra in all the range of modulation frequencies, while in our case the low-frequency pulse trains did not elicit this entrainment at the frequencies of 3, 7 and 13 Hz.

Spectral topographies revealed that the higher stimulation frequencies (19 Hz and 36 Hz) showed lateralization in the distribution of power across the scalp, indicating a higher entrainment of neurons in the contralateral side at the stimulation frequency, which was not observed in lower frequencies. It was expected to observe the maximum values of power across the scalp over the contralateral somatosensory cortex, around the left central and centroparietal electrodes. Even though this was not the case, the values in the somatosensory region were higher at the side contralateral to the stimulation than at the ipsilateral side. No further conclusions could be drawn from the spectral scalp topographies.

C. Effect of electrical artifact

An electrical artifact was observed in the data after every stimulation pulse at latencies ranging 0 to 6 ms after every pulse. This artifact did not affect analysis in the time domain, as this time range was not analyzed. In the frequency domain, it is expected that the artifact will appear in some way in the frequency spectra, and it may contribute to the visible peaks at the frequencies of stimulation by increasing their amplitude.

However, we have several reasons to believe that, even if the artifact may have contributed to the appearance of this peak, it is not its only source. First, SEP responses were observed in the time domain in this study, and spectral peaks have been observed at the frequency of stimulation by other researchers, as presented earlier in this discussion. Second, the artifact was present at every frequency of stimulation. If the only source of the spectral peak was the artifact, it should also be present at every frequency of stimulation, which was not the case. Third, spectral topographies showed a higher response contralateral to the side of stimulation. This lateralization could not be due to the artifact, as the artifact showed to be distributed across the scalp without any clear pattern. Finally, post-hoc analysis showed that, when the magnitude of the artifact was reduced by a 48% in average after re-referencing the data, the magnitude of the spectral peak was only reduced by a 17% in average. If the only source of the spectral peak was the artifact, the magnitude of this peak should have been reduced by the square of the magnitude, which was not the case.

All this being said, it is important to keep in mind that the artifact was present in the data, and it may have partially contributed to the amplitude of the spectral peaks at the stimulation frequencies. Preliminary results showed that removing the artifact during signal processing while not affecting the frequency spectra is a complicated task. Therefore, in order to increase the applicability of the methodology used in this study, the artifact should be fully reduced by further improving the experimental setup. Another alternative would be to use vibrotactile instead of electrical means to stimulate the somatosensory cortex. However, this modality also brings its own limitations.

D. Transition in the nature of the response

Transition to the so-called steady state was expected to be marked by a significant decrease in component amplitude, observable in the time domain, and a significant increase in power at the stimulated frequency, detectable by analysis in the frequency domain. Overall, our results showed consistency with this described transition for frequencies of 19 Hz and above when compared to lower frequencies.

Some previous research has hypothesized that these measurable differences arise simply due to the linear addition of the subsequent responses to individual stimuli. Our results indicates that the salient peak observed in the frequency spectra after stimulation at high frequencies was due to an oscillation that is different from the characteristic components observed in the transient SEP responses at lower frequencies. With these observations, and due to the complexity of the brain [43], we are inclined to interpret our results as an indication of a transition in the nature of the brain response. Following this hypothesis, the observed differences would be caused by the activation of neural pathways that oscillate synchronous to the stimulation, different to those activated at lower stimulation frequencies [40]. However, further research is needed to confirm this hypothesis.

E. Limitations and future work

This study was subject to some limitations which can be tackled in following studies in the same research line.

1) Assumption of stationarity: In both time and frequency domain approaches, results were obtained by averaging across the whole time period in which data was collected, either by direct averaging of the time response or by use of the Welch method, which is an indirect way of averaging. This approach assumes that the responses of the brain are stationary, while in reality they are not. Therefore, an average of the responses is obtained, potentially losing relevant information. Future studies could use time-frequency analyses to reveal processes related to e.g. attention or habituation to the stimulation.
2) Assumption of linearity: Both the time and frequency domain approaches used in this study assume that the system under investigation behaves as a linear system. However, it is safe to assume that the human brain is a complex nonlinear system. Presence of linear patterns like the ones observed in this study is useful as a first approach to understanding the behavior of the brain under certain circumstances, and it may prove useful under very specific experimental conditions like the ones presented here. However, more complex approaches are needed to expand the applicability of these results.
3) Peak detection: SEP components were labeled as such when maxima and minima were found around the expected latency. This approach may be limiting in the sense that any maxima/minima appearing at those latencies would be identified as a SEP component, when they could sometimes appear due to background

activity non-specific to the stimulation. Even though most background activity is expected to be removed by averaging, a more robust approach would also include some estimate of the SNR in the peak-detection algorithm. As an additional remark, it must be noted that, for the highest frequency of stimulation, the analysis period (50 ms) was longer than the stimulation period (27 ms), which could affect the detection of components. This is an inherent limitation of the analysis in the time domain. However, these peaks can still be used as a representation of the response, and therefore were not excluded from the analysis.

4) Limitations inherent to EEG: EEG is known for its high temporal resolution, which makes it possible to observe high-frequency components of the response like the ones present in this study. However, it provides low spatial resolution, making it hard to pinpoint the specific sources of the observed activity. Further research in the line of this study could use source localization methods to gain further insights about how stimulation frequency affects the generators of the SEP responses.
5) Limited stimulation frequencies: In this study, five different stimulation frequencies were used. Using a wider range of stimulation frequencies may bring further evidence to support the hypothesis that at high frequencies of stimulation, different cortical networks are activated. We recommend further exploration of frequencies in the beta band (12-30 Hz), as these have shown to elicit resonance-like properties in experiments with vibrotactile stimulation.
6) Stimulation with pulses: Periodic pulse trains were used in this study as stimulation signals. It must be noted that a pulse does not concentrate its energy at a single frequency. Instead, its power is distributed across the fundamental frequency and its higher harmonics, which reduces the proportion of power allocated to the fundamental component. In our study, stimulation with pure sinusoids was not feasible due to hardware limitations. However, sinusoidal stimulation would in principle concentrate nearly all power at the fundamental frequency, which may enhance the ability of the stimulation signal to drive and entrain network activity specifically at that frequency.
7) Number of participants: Data from eight healthy participants was analyzed in this study. Some trends were observed in the data that showed no statistical significance. Even though eight participants is a common amount in published studies in this field, we recommend repeating the analyses after collecting data from more participants, as this could provide new insights.

V. Conclusion

In this study, frequency domain analysis revealed that the stimulation frequency predominated in the EEG over adjacent frequencies for stimulation at 19 Hz and 36 Hz, and this was not the case for the lower frequencies of 3 Hz, 7 Hz and 13 Hz. Additionally, time domain analysis revealed that those higher frequencies presented a significantly lower amplitude of the P40 SEP component and less detectability of earlier characteristic SEP components when compared to the lowest stimulation frequency of 3 Hz. These results are consistent with previous definitions of a steady-state, which in our case was observed for frequencies of 19 Hz and higher. The cause of this transition could be a change in the nature of the brain response when the stimulation frequency is increased, which could involve activation of neural pathways different to those activated for lower frequencies. Further research is needed in order to confirm this hypothesis.

References

[1] O. N. Markand, *Clinical Evoked Potentials*. Springer International Publishing, 2020.

[2] L. Sornmo and P. Laguna, *Bioelectrical Signal Processing in Cardiac and Neurological Applications*. Elsevier, 2005.

[3] D. Regan, "Some characteristics of average steady-state and transient responses evoked by modulated light," *Electroencephalography and Clinical Neurophysiology*, vol. 20, pp. 238–248, 1966.

[4] F.-B. Vialatte, M. Maurice, J. Dauwels, and A. Cichocki, "Steady-state visually evoked potentials: Focus on essential paradigms and future perspectives," *Progress in Neurobiology*, vol. 90, pp. 418–438, 4 2010.

[5] T. W. Picton, J. Vajsar, R. Rodriguez, and K. B. Campbell, "Reliability estimates for steady-state evoked potentials," *Electroencephalography and Clinical Neurophysiology/Evoked Potentials Section*, vol. 68, pp. 119–131, 3 1987.

[6] T. W. Picton, M. S. John, A. Dimitrijevic, and D. Purcell, "Human auditory steady-state responses: Respuestas auditivas de estado estable en humanos," *International Journal of Audiology*, vol. 42, pp. 177–219, 1 2003.

[7] L. Zhang, W. Peng, Z. Zhang, and L. Hu, "Distinct features of auditory steady-state responses as compared to transient event-related potentials," *PLoS ONE*, vol. 8, 7 2013.

[8] G. Müller, C. Neuper, and G. Pfurtscheller, "Resonance-like frequencies of sensorimotor areas evoked by repetitive tactile stimulation," *Biomedizinische Technik*, vol. 46, pp. 186–190, 2001.

[9] A. Moungou, J. L. Thonnard, and A. Mouraux, "EEG frequency tagging to explore the cortical activity related to the tactile exploration of natural textures," *Scientific Reports*, vol. 6, 2 2016.

[10] S. Tobimatsu, M. Zhang, and M. Kato, "Steady-state vibration somatosensory evoked potentials: physiological characteristics and tuning function," *Clinical Neurophysiology*, vol. 110, pp. 1953–1958, 1999.

[11] E. Colon, S. Nozaradan, V. Legrain, and A. Mouraux, "Steady-state evoked potentials to tag specific components of nociceptive cortical processing," *NeuroImage*, vol. 60, pp. 571–581, 2012.

[12] A. Mouraux, G. Iannetti, E. Colon, S. Nozaradan, V. Legrain, and L. Plaghki, "Nociceptive steady-state evoked potentials elicited by rapid periodic thermal stimulation of cutaneous nociceptors," *Journal of Neuroscience*, vol. 31, pp. 6079–6087, 2011.

[13] X. Delberghe, N. Mavroudakis, D. Zegers De Beyl, and E. Brunko, "The effect of stimulus frequency on post-and pre-central short-latency somatosensory evoked potentials (SEPs)," *Electroencephalography and clinical Neurophysiology*, vol. 77, pp. 86–92, 1990.

[14] G. Abbruzzese, D. Dall'Agata, M. Morena, L. Reni, G. Trivelli, and E. Favale, *Selective Effects of Repetition Rate on Frontal and Parietal Somatosensory Evoked Potentials (SEPs)*. Elsevier, 1990, pp. 145–148.

[15] L. G. Larrea, H. Bastuji, and F. Mauguière, "Unmasking of cortical SEP components by changes in stimulus rate: a topographic study," *Electroencephalography and Clinical Neurophysiology/ Evoked Potentials*, vol. 84, pp. 71–83, 1992.

[16] N. S. Namerow, R. J. Sclabassi, and N. F. Enns, "Somatosensory response to stimulus trains: Normative data," *Electroencephalography and Clinical Neurophysiology*, vol. 37, pp. 11–21, 1974.

[17] R. Noss, C. Boles, and C. Yingling, "Steady-state analysis of somatosensory evoked potentials," *Electroencephalography and Clinical Neurophysiology - Evoked Potentials*, vol. 100, pp. 453–461, 1996.

[18] F. Mina, V. Attina, Y. Duroc, E. Veuillet, E. Truy, and H. Thai-Van, "Auditory steady state responses and cochlear implants: Modeling the artifact-response mixture in the perspective of denoising," *PLoS ONE*, vol. 12, 2017.

[19] B. van den Berg, M. Manoochehri, M. Kasting, A. Schouten, F. van der Helm, and J. Buitenweg, "Multisine frequency modulation of intraepidermal electric pulse sequences: A novel tool to study nociceptive processing," *Journal of Neuroscience Methods*, vol. 353, 2021.

[20] T. D. Sanger, A. Pascual-Leone, D. Tarsy, and G. Schlaug, "Nonlinear sensory cortex response to simultaneous tactile stimuli in writer's cramp," vol. 17, no. 1, pp. 105–111, 1 2002.

[21] M. Tinazzi, A. Priori, L. Bertolasi, E. Frasson, F. Mauguiè, and A. Fiaschi, "Abnormal central integration of a dual somatosensory input in dystonia Evidence for sensory overflow," vol. 123, pp. 42–50, 2000.

[22] T. Nyrke and A. Lang, "Spectral analysis of visual potentials evoked by sine wave modulated light in migraine," *Electroencephalography and Clinical Neurophysiology*, vol. 53, no. 4, pp. 436–442, 4 1982.

[23] S. Kalitzin, J. Parra, D. N. Velis, and F. H. Lopes Da Silva, "Enhancement of phase clustering in the EEG/MEG gamma frequency band anticipates transitions to paroxysmal epileptiform activity in epileptic patients with known visual sensitivity," *IEEE Transactions on Biomedical Engineering*, vol. 49, no. 11, pp. 1279–1286, 11 2002.

[24] A. Gevins, J. Le, N. K. Martin, P. Brickett, J. Desmond, and B. Reutter, "High resolution eeg: 124-channel recording, spatial deblurring and mri integration methods," *Electroencephalography and Clinical Neurophysiology*, vol. 90, pp. 337–358, 5 1994.

[25] E. Meyers, M. Alves, A. Teugels, and D. Torta, "No evidence that working memory modulates the plasticity of the nociceptive system, as measured by secondary mechanical hypersensitivity," *Journal of Pain*, vol. 24, pp. 1931–1945, 2023.

[26] E. Diesch, H. Preissl, M. Haerle, H.-E. Schaller, and N. Birbaumer, "Multiple frequency steady-state evoked magnetic field mapping of digit representation in primary somatosensory cortex," *Somatosensory and Motor Research*, vol. 18, pp. 10–18, 2001.

[27] A. Delorme and S. Makeig, "EEGLAB: an open source toolbox for analysis of single-trial eeg dynamics including independent component analysis," *Journal of Neuroscience Methods*, vol. 134, pp. 9–21, 3 2004.

[28] T. Yamada, M. Yeh, and J. Kimura, "Fundamental principles of somatosensory evoked potentials," pp. 19–42, 2004.

[29] L. G. Larrea, H. Bastuji, and F. Mauguière, "Unmasking of cortical sep components by changes in stimulus rate: a topographic study," *Electroencephalography and Clinical Neurophysiology/ Evoked Potentials*, vol. 84, pp. 71–83, 1992.

[30] C.-L. Yeh, P.-L. Lee, W.-M. Chen, Y.-T. Wu, and G.-Y. Lan, "Improvement of classification accuracy in a phase-tagged steady-state visual evoked potential-based brain computer interface using multiclass support vector machine," *Biomedical engineering online*, vol. 12, p. 46, 05 2013.

[31] J. L. Parker, N. H. Shariati, and D. M. Karantonis, "Electrically evoked compound action potential recording in peripheral nerves," *Bioelectronics in Medicine*, vol. 1, pp. 71–83, 1 2018.

[32] A. Eisen, "The somatosensory evoked potential," *Canadian Journal of Neurological Sciences / Journal Canadien des Sciences Neurologiques*, vol. 9, pp. 65–77, 1982.

[33] H. Pratt, D. Politoske, and A. Starr, "Mechanically and electrically evoked somatosensory potentials in humans: Effects of stimulus presentation rate," *Electroencephalography and Clinical Neurophysiology*, vol. 49, pp. 240–249, 1980.

[34] T. Allison, G. McCarthy, C. C. Wood, and S. J. Jones, "Potentials evoked in human and monkey cerebral cortex by stimulation of the median nerve," *Brain*, vol. 114, pp. 2465–2503, 1991. [Online]. Available: https://academic.oup.com/brain/article-lookup/doi/10.1093/brain/114.6.2465

[35] S. Gandevia, D. Burke, and B. M. Keon, "The projection of muscle afferents from the hand to cerebral cortex in man," *Brain*, vol. 107, pp. 1–13, 1984.

[36] E. Kunesch, S. Knecht, A. Schnitzler, C. Tyercha, F. Schmitz, and H. J. Freund, "Somatosensory evoked potentials elicited by intraneural microstimulation of afferent nerve fibers," *Journal of Clinical Neurophysiology*, vol. 12, pp. 476–487, 9 1995.

[37] H. Steinmetz, G. Fürst, and B.-U. Meyer, "Craniocerebral topography within the international 10–20 system," *Electroencephalography and Clinical Neurophysiology*, vol. 72, pp. 499–506, 6 1989.

[38] M. Okamoto, H. Dan, K. Sakamoto, K. Takeo, K. Shimizu, S. Kohno, I. Oda, S. Isobe, T. Suzuki, K. Kohyama, and I. Dan, "Three-dimensional probabilistic anatomical cranio-cerebral correlation via the international 10–20 system oriented for transcranial functional brain mapping," *NeuroImage*, vol. 21, pp. 99–111, 1 2004.

[39] R. Kessler and S. P. Heinrich, "Temporal frequency dependence of the polarity inversion between upper and lower visual field in the pattern-onset steady-state visual evoked potential," *Documenta Ophthalmologica*, vol. 146, pp. 53–63, 2 2023.

[40] C. S. Herrmann, "Human eeg responses to 1-100 hz flicker: Resonance phenomena in visual cortex and their potential correlation to cognitive phenomena," *Experimental Brain Research*, vol. 137, pp. 346–353, 2001.

[41] A. Z. Snyder, "Steady-state vibration evoked potentials: description of technique and characterization of responses," *Electroencephalography and Clinical Neurophysiology/ Evoked Potentials*, vol. 84, pp. 257–268, 1992.

[42] S. Su, G. Chai, X. Sheng, and X. Zhu, "Electrical stimulation-induced sssep as an objective index for the evaluation of sensory ability," in *International IEEE/EMBS Conference on Neural Engineering, NER*, vol. 2019-March, 2019, pp. 908–911.

[43] W. Klonowski, "Everything you wanted to ask about EEG but were afraid to get the right answer," *Nonlinear Biomedical Physics*, vol. 3, 5 2009.

[44] O. G. Filatova, Y. Yang, J. P. Dewald, R. Tian, P. Maceira-Elvira, Y. Takeda, G. Kwakkel, O. Yamashita, and F. C. van der Helm, "Dynamic information flow based on EEG and diffusion MRI in stroke: A proof-of-principle study," *Frontiers in Neural Circuits*, vol. 12, 10 2018.

APPENDIX A
PILOT TESTS

Before conducting the formal experiment, different pilot tests were conducted to determine the final experimental setup and procedure. This appendix presents choices that were made and the reasoning behind them, as well as the procedure and preliminary results from the tests.

A. *Choice of stimulation signals.*

For study of steady-state responses in the frequency domain, the ideal stimulation signal would focus all the power at one or several frequencies of choice. Following this criterion, four signals were compared:

1) pulse train (PT)
2) pulse train modulated in amplitude by a sine (AM)
3) pulse train modulated in amplitude by a boxcar function (BM)
4) pulse-position-modulated pulse train (PPM)

These signals were generated in Matlab with a sampling frequency of 1,024 Hz. The pulse train had a pulse frequency of 3 Hz. The amplitude-modulated pulse trains had a modulation frequency of 3 Hz and a carrier frequency of 150 Hz. The pulse-position modulated signal was obtained by optimization of the pulse position to achieve the maximum power at the frequency of 3 Hz. The space between pulses was constrained to the range 5-50 ms, to mimic a firing frequency of 20-200 Hz. The power spectral density (PSD) of each signal was calculated in Matlab and they were compared.

All the signals and their power spectra are displayed in Fig. 11. The power of each signal at the frequency of 3 Hz is displayed in Fig. 12. The signal with more power at the frequency of 3 Hz is the pulse train modulated in amplitude with a sinusoid (AM). Then follow the pulse-position-modulated pulse train (PPM) and the amplitude-modulated pulse train by a boxcar function (BM). Lastly, the pulse train (PT) as the lowest power at 3 Hz.

The AM signal was discarded due to limitations in the available equipment, and the PPM signal was selected for the pilot tests for being the second signal with the highest power at 3 Hz and for distributing the power at higher frequencies among a wide range of frequencies, instead of focusing it at specific frequencies.

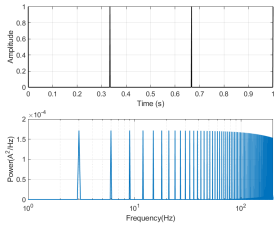

(a) Pulse train (PT). Pulse frequency: 3 Hz.

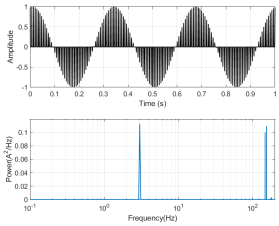

(b) Pulse train, modulated in amplitude with a sinusoid (AM) Modulation frequency: 3 Hz. Carrier frequency: 150 Hz.

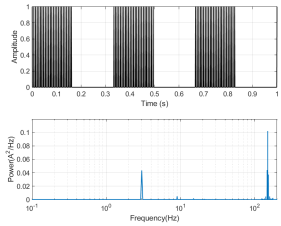

(c) Pulse train, modulated in amplitude with a boxcar function (BM). Modulation frequency: 3 Hz. Carrier frequency: 150 Hz.

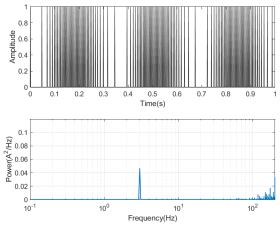

(d) Pulse-position modulated pulse train (PPM).

Fig. 11: Four different stimulation signals and their frequency spectra, generated in Matlab with a sampling frequency of 1,024 Hz.

B. *Choice of electrodes*

During initial tests, two spherical electrodes placed 2.5 cm apart were used to deliver electrical stimulation to the median nerve at the wrist, like the ones depicted in Fig. 13a. These electrodes enable a small contact surface on the skin, through which all the current is delivered. The perception threshold for the electrical stimulation was found to be 0.3 mA, 0.5 mA and 0.5 mA for the three tested subjects. The amplitude used for stimulation was 1.5 times the perception threshold. The subjects reported to feel discomfort and one reported a pain sensation after half an hour of discontinued stimulation. After the experiments, two of the subjects had a small burn mark on the skin at the location of the electrodes, which lasted over a week. For these reasons, it was decided to use electrodes for transcutaneous electrical nerve stimulation (TENS) instead, like the ones in Fig 13b. The perception threshold for TENS electrodes was higher, indicating that there is less transmission of the current to the nerves. However, these electrodes did not generate sensations of pain and they did not leave any mark on the skin of the subjects. Therefore, they were chosen for the formal experiment.

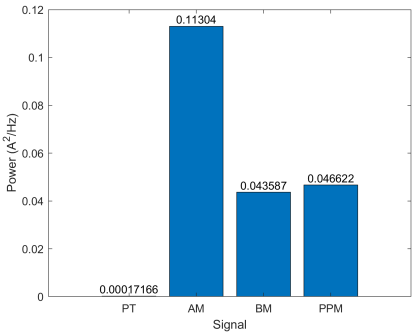

Fig. 12: Power at 3 Hz for each of the four signals.

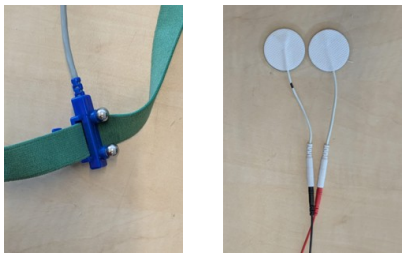

(a) Spherical electrodes

(b) TENS electrodes

Fig. 13: Two types of electrodes used for delivering electrical stimulation. (a) Spherical electrodes used during pilot tests. (b) TENS electrodes used during formal experiment.

C. Pilot test procedure

The objective of this test was to validate the procedure to evoke SSEPs, by observing peaks in the frequency spectra at the stimulation frequencies. The participant was one healthy adult, male, right-handed, with no history of neurological disorders or implanted electronic medical devices.

The subject was seated in a chair, on a comfortable position in a dim, silent room and asked to relax. Transcutaneous electrical stimulation was delivered at the wrist through two spherical electrodes 2.5 cm apart (Fig. 13a) using Micromed Energy stimulator (constant current stimulator). The stimulation signal had the shape of pulse trains, modulated by a sinusoid with pulse position modulation (PPM), similar to the one in Fig. 11d. Modulation frequencies were 13 Hz, 23 Hz and 43 Hz. In previous studies, when modulated signals were used, carrier frequency was at least 150 Hz [17] [26] [12] [11]. In this case, the carrier frequency was 150 Hz.

The participant received stimulation in 6 blocks, each with a duration of 120 s (2 min) and a rest period of 2 min after each block. In each block (which had 6 stimulation trains), each of the 3 frequencies was repeated twice, in pseudorandom order. Each block was made of 10 s trains of stimulation, followed by 10 s inter-train intervals (no stimulation). Each train had one single frequency. In half of the trains, the pulse width was 0.5 ms, while in the other half it was 1 ms. This block design was inspired by the one adopted in previous studies [12] [11].

EEG was measured with a 64-electrode cap from TMSi (Infitiny Gel model). Epochs corresponding to stimulation at each of the frequencies were extracted. Then, power spectral density was calculated and averaged across all channels. Power values at the stimulation frequency were extracted for each channel, frequency of stimulation and pulse width.

D. Preliminary results

The PSD was calculated for epochs with stimulation at each of the three frequencies. Fig. 14 shows all-channel averages. For each of the stimulation frequencies, we can see clear peaks in the power at frequencies near the stimulation frequency. We can also observe some smaller peaks near their harmonics (Fig. 14a 14b) and subharmonics (Fig. 14b).

The value of the PSD at the frequency of 3 Hz was extracted and compared between pulse widths of 0.5 ms and 1 ms for each stimulation frequency. For the three stimulation frequencies, the power at the frequency of interest was higher when the pulse width was larger (1 ms versus 0.5 ms).

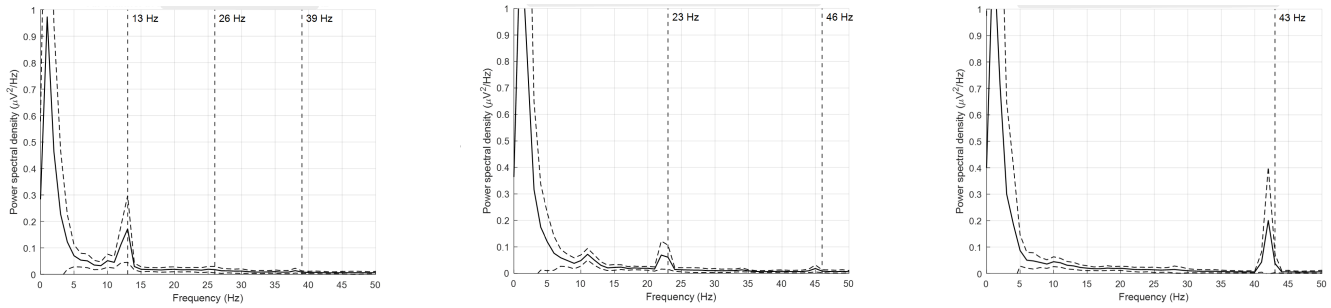

(a) Stimulation at 13 Hz (b) Stimulation at 23 Hz (c) Stimulation at 43 Hz

Fig. 14: Average across all channels of the power spectral density. Epochs with each stimulation frequency were analyzed separately. Vertical dashed lines indicate stimulation frequencies and their harmonics.

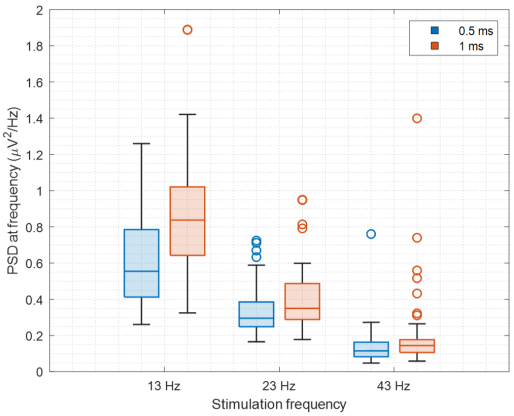

Fig. 15: Power at the stimulation frequency for each stimulation frequency and pulse width (0.5 ms or 1 ms), across all channels.

Analysis of the collected data in the time domain revealed an electrical artifact after every stimulation pulse, with amplitudes up to 40 μV.

E. Discussion of results

Preliminary tests showed peak at the stimulation frequencies and their harmonics, as expected. However, it was found that every stimulation pulse generated an electrical artifact of high magnitude. It was hypothesized that artifact may increase the power at the stimulation frequencies, hindering the analysis of the cortical response in the frequency domain. Therefore, further investigation was needed in order to reduce the magnitude and presence of this artifact.

F. Conclusions from the pilot tests

Four main conclusions were obtained from the pilot tests:

1) Spherical electrodes generated an undesired sensation of pain and they sometimes left a burn mark on the skin. Other choice of electrodes is preferable.
2) There was an artifact in the collected data. Ways to reduce this artifact must be explored, both in the experimental setup (hardware) and in the signal processing (software).
3) Modulated signals effectively focused the power at modulation frequencies and reduced the power at their harmonics. However, short duration of the period between consecutive pulses makes it hard to interpret the response to individual pulses.

G. Further tests and reduction of artifact

Further tests (not presented in this report) identified the main source of the artifact, which was the cable connecting the stimulator with the stimulating electrodes. It was hypothesized that this cable was acting as an antenna, generating an electromagnetic interference (EMI) which was captured by the electrodes in the EEG cap. The magnitude of the artifact was effectively reduced by shielding these cables with a copper braided mesh, connected to the laboratory ground. This provided a low-resistance path for the EMI, reducing its appearance in the recorded data.

APPENDIX B
ARTIFACT CORRECTION WITH SIMPLE METHODS IN SIMULATED DATA

This appendix presents exploratory analyses in which the effect of different techniques for artifact removal on the frequency spectrum were evaluated. This was done using a simulated artifactual signal, which was created by adding an artificial artifact to a baseline EEG recording. None of the methods explored showed to consistently reduce the magnitude of the artifact as it was expected.

A. Background

Electrical stimulation results in an electrical artifact after every stimulation pulse. This artifact may increase the magnitude of the peak at the frequency of interest in the power spectrum. This makes it hard to know the actual magnitude of the brain response at this frequency. If the data is analyzed in the time domain, the artifact can be removed by applying a blanking window [44]. However, applying a blanking window will increase the power at that frequency, which will increase the peak in the PSD. Therefore, an alternative method for artifact removal is needed for frequency-domain analysis.

B. Methods

By simulating an EEG signal, we can evaluate the effect of different artifact removal methods on the power spectrum. EEG baseline data from one subject was used to generate the simulated signal. These data had been recorded during the formal experiment, of which conditions are described in Section II-B. An artificial artifact was inserted at the frequency of 37 Hz, by adding the magnitudes of - 5 μV and +5μV in two consecutive samples at that frequency. Then, this artifact was eliminated from the data, in the time range [-1, 4] ms around the start of the artifact, with four different methods:

1) "Interp + noise". Data in the removed time window was interpolated using Matlab's "pchip" interpolation (C^1 continuity, ensuring smooth transition between segments). Then, noise was added by adding randomly drawn values from a standard normal distribution. This was done in order to replicate random noise from EEG data.
2) "Interp". Data in the removed time window was linearly interpolated.
3) "Substitution". Data in the removed time window was substituted by previous data in the signal. Data for substitution was drawn from a window of the same length as the removed data, where the last sample was 0 to 5 samples (number chosen at random) before the first sample in the removed data.
4) "Removal". Data in the removed time window was not substituted by other data.

Fig. 16 (top) illustrates the resulting signals by showing one single peak generated by the artifact. The power spectral density (PSD) was calculated for each of the resulting signals using Welch's overlapped segment averaging estimator (Matlab's "pwelch") with a Hamming window of size equal to the sampling rate (in order to get a 1 Hz resolution). The resulting spectra were baseline corrected by subtracting the PSD from the original baseline signal.

We expect that, by adding the artificial artifact, there will be an increase in power at the frequency of the artifact and its harmonics. This should be visible as peaks at those values in the baseline-corrected PSD. Then, after removing the artifact with any of the four methods, a decrease in the magnitude of the peak at the stimulation frequency would confirm that the methods have the expected effect.

For each removal method, the absolute value of the PSD at the stimulation frequency was extracted and compared to the other methods. Then, from this value, the average of the adjacent frequencies (one above and one below) were removed. This allowed to evaluate the amplitude of the peaks at those values. This value was also compared within methods. The same

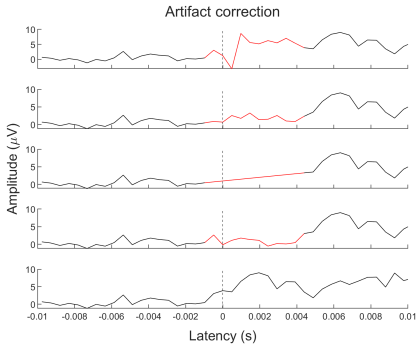

Fig. 16: Artifact before and after correction. From top to bottom: Artifact and correction methods 1, 2, 3 and 4.

procedure was then repeated for the frequencies of 3 Hz, 7 Hz, 13 Hz and 19 Hz.

C. Results

Adding the artifact to the signal generated peaks in the PSD at the frequency of stimulation and its harmonics, as expected (blue line in Fig. 17a) . All the correction methods reduced the amplitude of the peaks at the higher harmonics. However, they increased the power at low frequencies, as seen in Fig. 17a.

An evaluation of baseline-corrected power of the signal with artifact and after applying the different correction methods can be done based on Fig. 17. It shows the data for different (simulated) stimulation frequencies, both in absolute value and relative to adjacent frequencies. In the signal with artifact, the power has a magnitude in the order of 10^{-5} at the frequency of stimulation for stimulation frequencies of 3 Hz, 7 Hz, 13 Hz and 19 Hz, and a power of the order of 10^{-4} for stimulation frequency of 37 Hz. These bars can barely be seen in Fig. 17. If the correction methods worked as expected, the bars for all the correction methods would be smaller than the "Artifact" bar. However, because this is not the case, it can be said that none of these methods showed to consistently reduce the magnitude of the artifact in the frequency spectrum.

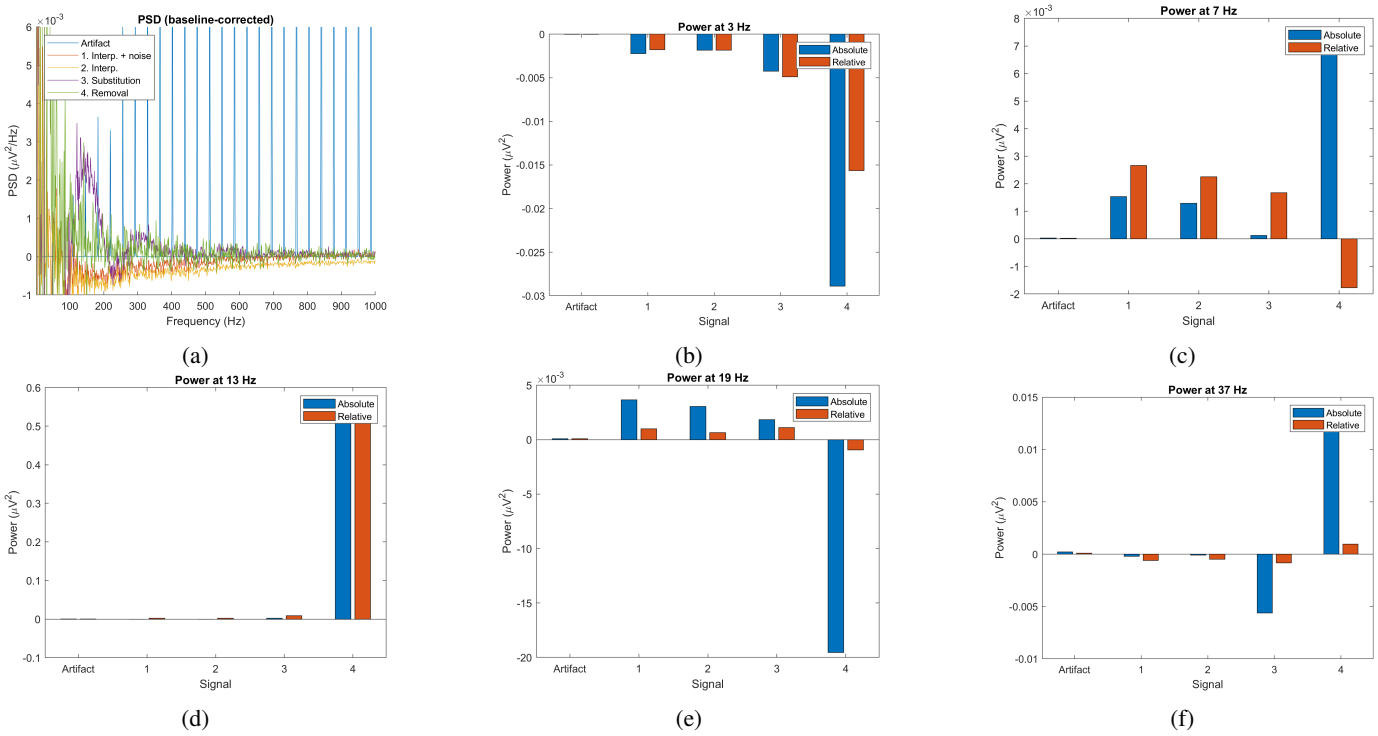

Fig. 17: (a) Baseline-corrected power spectral density of the signal before removing the simulated artifact and after removing it with each of the four methods, for a stimulation frequency of 37 Hz. (b-f) Baseline-corrected power at the frequency of interest. Value is presented for the signal with artifact and after applying the different correction methods, both in absolute value and relative to adjacent frequencies. Results for different simulated frequencies are presented. The correction methods are: 1. "Interp + noise" , 2. "Interp", 3. "Substitution" and 4. "Removal".

D. Conclusion

Even though these simple methods can be useful to reduce electrical artifact in the time domain, they do not show to consistently eliminate the effect of artifact in the frequency domain. Other methods should be explored to remove this artifact from the data.

APPENDIX C
SEPS FOR EVERY SUBJECT AND FREQUENCY

This appendix presents the individual SEP waveforms and detected components for every subject. These are displayed in Fig. 18. Every row corresponds to one subject, and every column corresponds to one stimulation frequency (3 Hz, 7 Hz, 13 Hz, 19 Hz and 36 Hz).

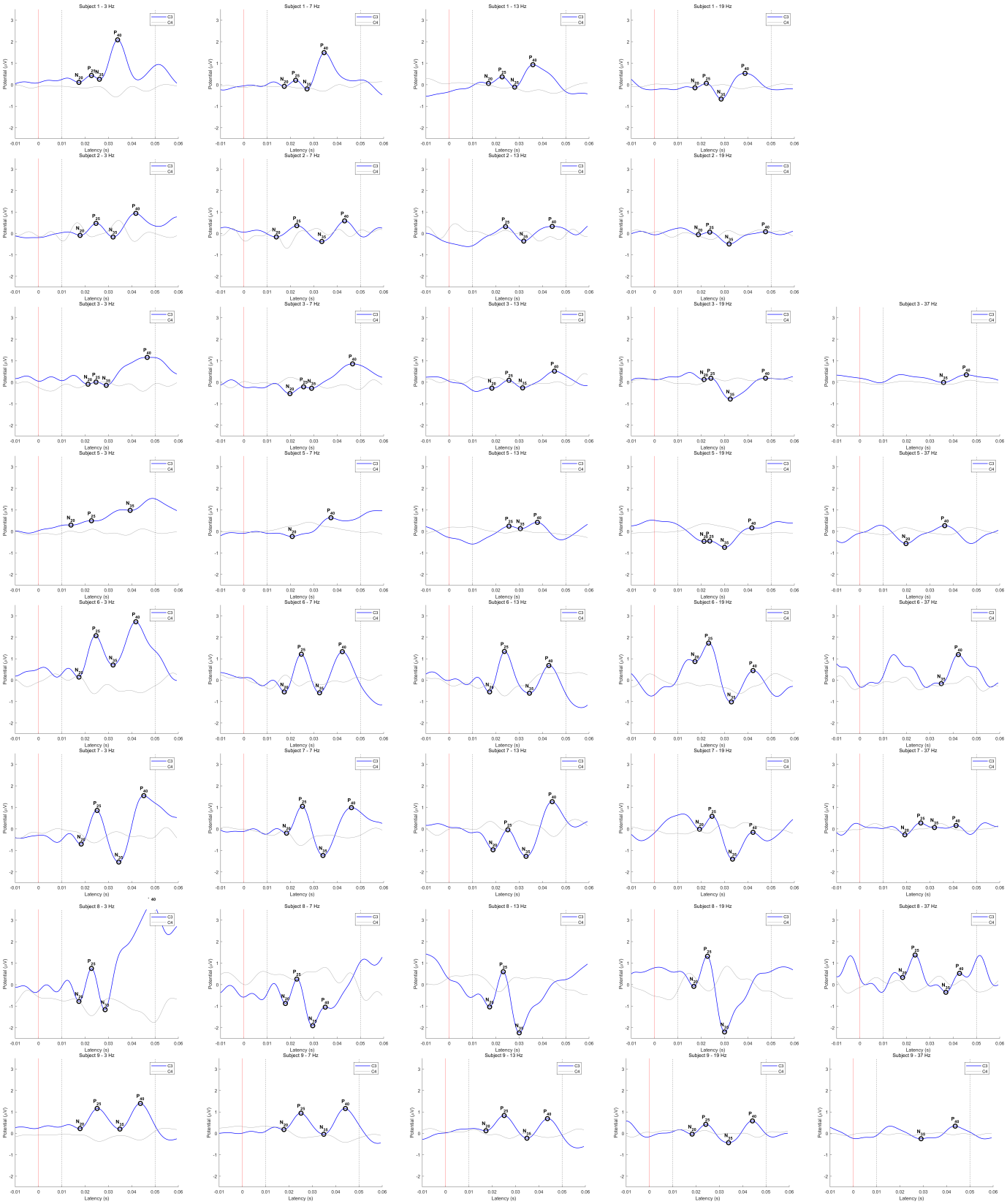

Fig. 18: Somatosensory evoked potential (SEP). Figures display the average across >1,000 epochs for each subject (rows) and frequency (columns, in this order: 3 Hz, 7 Hz, 13 Hz, 19 Hz and 37 Hz). Characteristic SEP features are marked with an 'o'.

APPENDIX D
STATISTICAL ANALYSIS

This section presents the detailed procedure and results of the statistical analysis tests presented in the main text.

A. Amplitude data

Statistical analyses were performed to test differences in peak amplitude between the different stimulation frequencies using IBM SPSS Statistics (Version 29.0).

In order to use parametric tests like the commonly used ANOVA [11] [14], data must fulfill the criterion of normality. To test whether the data follows a normal distribution, the Shapiro-Wilk was used. In this test, the null hypothesis is that the sample is drawn from a normally-distributed population. Shapiro-Wilk tests were performed for every peak and frequency of stimulation.

Table V displays the results of the Shapiro-Wilk test. In this table, W is the test statistic which ranges from 0 to 1 with a value closer to 1 indicating that the distribution resembles more a normal distribution. The p value is the probability of obtaining a W statistic as extreme as the one observed, assuming the data actually comes from a normal distribution. In the cases where $p \leq \alpha$, the null hypothesis is rejected and we can assume that data does not come from a normal distribution.

In each of the four peaks, for at least one of the frequencies, either a Shapiro-Wilk test rejected normality (α = 0.05) or the number of samples was too small to perform the test or assume a normal distribution ($n \leq 3$). Therefore, it was concluded that a parametric test was not appropriate for the data.

TABLE V: Shapiro–Wilk normality test results for amplitudes .

Peak	Frequency	W	p-value	Result (α = 0.05)
1	1	0.8256	0.0727	Fail to reject normality
	2	0.9768	0.9425	Fail to reject normality
	3	0.9014	0.3822	Fail to reject normality
	4	0.7712	0.0177	**Reject normality**
	5	0.9603	0.6171	Fail to reject normality
2	1	0.9303	0.5538	Fail to reject normality
	2	0.9062	0.4119	Fail to reject normality
	3	0.9240	0.4628	Fail to reject normality
	4	0.9269	0.4887	Fail to reject normality
	5	-	-	**n < 3**
3	1	0.9305	0.5203	Fail to reject normality
	2	0.9343	0.5564	Fail to reject normality
	3	0.8206	0.0462	**Reject normality**
	4	0.8328	0.0593	Fail to reject normality
	5	0.9440	0.6945	Fail to reject normality
4	1	0.8766	0.1747	Fail to reject normality
	2	0.9873	0.9899	Fail to reject normality
	3	0.9338	0.5833	Fail to reject normality
	4	0.9755	0.9373	Fail to reject normality
	5	0.7806	0.0391	**Reject normality**

Friedman tests were used as a non-parametric alternative to one-way repeated measures ANOVA. Friedman's test is used to test differences between three or more conditions when the measures are related. In this case they are, because every subject was stimulated with each frequency. The Friedman test's χ^2 statistic quantifies how much the summed ranks per condition deviate from what would be expected under the null hypothesis of equal medians.

The results are reported in Table VI. For peaks 1 and 2, only 4 conditions were included (frequencies 1 to 4), as data was insufficient to run the test for the highest frequency. This is reflected in the degrees of freedom of the test. All 5 conditions were included in peaks 4 and 5.

TABLE VI: Friedman test results for differences in amplitude per frequency, for each peak.

Peak	χ^2(df)	p-value	Result (α = 0.05)
1	5.000 (3)	0.1718	No significant difference
2	3.800 (3)	0.2839	No significant difference
3	10.080 (4)	0.0391	**Significant difference**
4	17.760 (4)	0.0014	**Significant difference**

For the amplitude of peaks 1 and 2, no significant difference was found among stimulation frequencies. A significant difference was found the amplitude of peaks 3 and 4 among stimulation frequencies. Post-hoc pairwise comparison tests were performed in the two statistically significant cases, with Bonferroni correction for multiple tests, to test which specific conditions (frequencies) showed this difference.

Results of post-hoc pairwise comparisons are displayed in Table VII. For peak 3, after applying the Bonferroni correction for multiple tests, no statistically significant differences were found for any of the pairwise comparisons. For peak 4, statistically

TABLE VII: Post-hoc test results for difference in amplitude in Peaks 3 and 4.

Peak	Comparison	Test statistic	Significance	Significance adjusted (Bonferroni)
Peak 3	f4-f3	1.000	0.317	1.000
	f4-f2	1.800	0.072	0.719
	f4-f1	2.400	0.016	0.164
	f4-f5	-2.800	0.005	0.051
	f3-f2	0.800	0.424	1.000
	f3-f1	1.400	0.162	1.000
	f3-f5	-1.800	0.072	0.719
	f2-f1	0.600	0.549	1.000
	f2-f5	-1.000	0.317	1.000
	f1-f5	-0.400	0.689	1.000
Peak 4	f4-f5	-0.800	0.424	1.000
	f4-f3	1.800	0.072	0.719
	f4-f2	2.600	0.009	0.093
	f4-f1	3.800	0.000	**0.001**
	f5-f3	1.000	0.317	1.000
	f5-f2	1.800	0.072	0.719
	f5-f1	3.000	0.003	**0.027**
	f3-f2	0.800	0.424	1.000
	f3-f1	2.000	0.046	0.455
	f2-f1	1.200	0.230	1.000

significant differences were found between frequency 1 and 4 (T=3.8, p=0.001) and between frequencies 1 and 5 (T=3, p=0.027).

B. Latency data

The same procedure and rationale followed for amplitude data as explained in the previous paragraphs (Appendix D-A) was also followed for latency data. A summary of the results is presented in the main text (Section III-B). All the results of the Shapiro-Wilk test are presented in Table VIII and all the results of the Friedman test are presented in Table IX of this Appendix.

TABLE VIII: Shapiro–Wilk normality test results for latencies.

Peak	Frequency	W	p-value	Result (α = 0.05)
1	1	0.8095	0.0370	**Reject normality**
	2	0.8875	0.1908	Fail to reject normality
	3	0.8663	0.2117	Fail to reject normality
	4	0.8868	0.2184	Fail to reject normality
	5	0.9643	0.6369	Fail to reject normality
2	1	0.7511	0.0084	**Reject normality**
	2	0.8425	0.1048	Fail to reject normality
	3	0.9006	0.2929	Fail to reject normality
	4	0.9590	0.8006	Fail to reject normality
	5	-	-	**n < 3**
3	1	0.9723	0.9157	Fail to reject normality
	2	0.9242	0.5027	Fail to reject normality
	3	0.9752	0.9351	Fail to reject normality
	4	0.9227	0.4524	Fail to reject normality
	5	0.9222	0.5443	Fail to reject normality
4	1	0.8975	0.2774	Fail to reject normality
	2	0.8835	0.2033	Fail to reject normality
	3	0.8059	0.0468	**Reject normality**
	4	0.9081	0.3832	Fail to reject normality
	5	0.9144	0.4662	Fail to reject normality

TABLE IX: Friedman test results for differences in latency per frequency, for each peak .

Peak	χ^2(df)	p-value	Result (α = 0.05)
1	3.643 (3)	0.3027	No significant difference
2	10.722 (3)	0.0133	**Significant difference**
3	1.277 (4)	0.8653	No significant difference
4	4.743 (4)	0.3147	No significant difference

TABLE X: Post-hoc test results for difference in latency in Peak 2.

Peak	Comparison	Test statistic	Significance	Significance adjusted (Bonferroni)
Peak 2	f4-f2	2.588	0.010	0.058
	f4-f1	2.381	0.017	0.104
	f4-f3	1.656	0.098	0.586
	f2-f1	0.725	0.469	1.000
	f2-f3	-0.932	0.352	1.000
	f1-f3	-0.207	0.836	1.000

C. SNR data

Statistical analyses were performed to tests whether SNR at each frequency of stimulation was different from zero. An additional analysis was used to test whether the SNR at F4 and F5 was different.

Signal-to-noise data was tested for normality in each of the groups (each of the stimulation frequencies), to select an adequate statistical tests. A Shapiro-Wilk test, of which results are displayed in Table XI, rejected normality in 3 out of the 6 groups. Therefore, non-parametric tests were used for further analysis.

A one sample Wilcoxon signed-rank test was used to compare the medians of each group with the value zero. For this test, the null hypothesis is that the median of the tested sample is equal to zero. Results for this test are displayed in Table XII. For frequencies F1, F2 and F3, no significant difference was found between the value of the SNR and zero. For frequencies F4 and F5, the SNR was found to be significantly different from zero. Another Wilcoxon signed-rank test was used to compare the median SNR at F4 and F5, of which results are displayed in Table XIII. The null hypothesis for this test is that the median of the difference between these two groups is equal to zero. This test concluded that there was no significant difference in SNR between F4 and F5.

TABLE XI: Shapiro–Wilk normality test results for SNR.

Frequency	W	p-value	Result (α = 0.05)
1	0.591	$<$0.001	**Reject normality**
2	0.819	0.087	Fail to reject normality
3	0.630	0.001	**Reject normality**
4	0.908	0.422	Fail to reject normality
5	0.791	0.049	**Reject normality**

TABLE XII: Wilcoxon signed-rank test results for SNR at each frequency against zero.

Frequency	W	p-value	Result (α = 0.05)
1	7	0.123	No significant difference
2	12	0.401	No significant difference
3	14	0.575	No significant difference
4	26	0.043	**Significant difference**
5	21	0.028	**Significant difference**

TABLE XIII: Wilcoxon signed-rank test results for SNR comparison between F4 and F5.

Comparison	W	p-value	Result (α = 0.05)
f4-f5	19	0.075	No significant difference

APPENDIX E
ARTIFACT ANALYSIS

This appendix presents some of the figures that were used to investigate the presence of the electrical artifact, its shape, magnitude and topography across all subjects.

A. Methods

An artifact analysis was performed to evaluate the shape and magnitude of the electrical artifact caused by electrical stimulation that was present in the collected data. Continuous data were high-pass filtered at 1 Hz to remove slow drifts. Epochs were extracted time-locked to every stimulation pulse, in the time range 11 ms before every pulse to 11 ms after every pulse. Time series data were averaged across all collected epochs for each subject (>4,000 epochs) to visualize the average magnitude in each channel and the topography of the artifact. These data were displayed in a time-topography plot for each of the subjects.

B. Results

Average across epochs was plotted for every channel and for each subject, along with the topography at the time of maximum amplitude. Results for all the subjects are presented in Fig. 19.

Artifact topographies varied across subjects. In three of the subjects (subjects 1, 7 and 9), the extremum at the represented latency was recorded in the right parieto-occipital area, mostly on electrode PO6. In one of the subjects (subject 8), it was in the frontmost central electrode, Fpz. One subject (subject 6) showed maxima at both fronto-central and parieto-occipital electrodes (Fpz and O2). Another subject (subject 5) showed a maximum in the fronto-central area, located around electrode FC1. The two remaining subjects (subjects 2 and 3) showed a more disperse topography, with several maxima and minima across the scalp.

C. Further insights

The topographies that show a clear extremum rather than several maxima and minima correspond to those in which one channel has an artifact with a magnitude much bigger than the rest of the channels, as can be seen in the Potential vs. Latency plots in Fig.19. For example, in the most representative case of this effect (subject 9), one of the electrodes recorded an artifact with a peak amplitude above 40 μV, while in all the rest of the channels the peak value was below 8 μV in absolute value. When removing the channel or channels with the highest amplitudes, these topographies also showed more dispersion across all the remaining electrodes.

D. Results of post-hoc artifact analysis

Fig. 20 presents the results described in the main text for the post-hoc artifact analysis, for each individual subject and across all subjects.

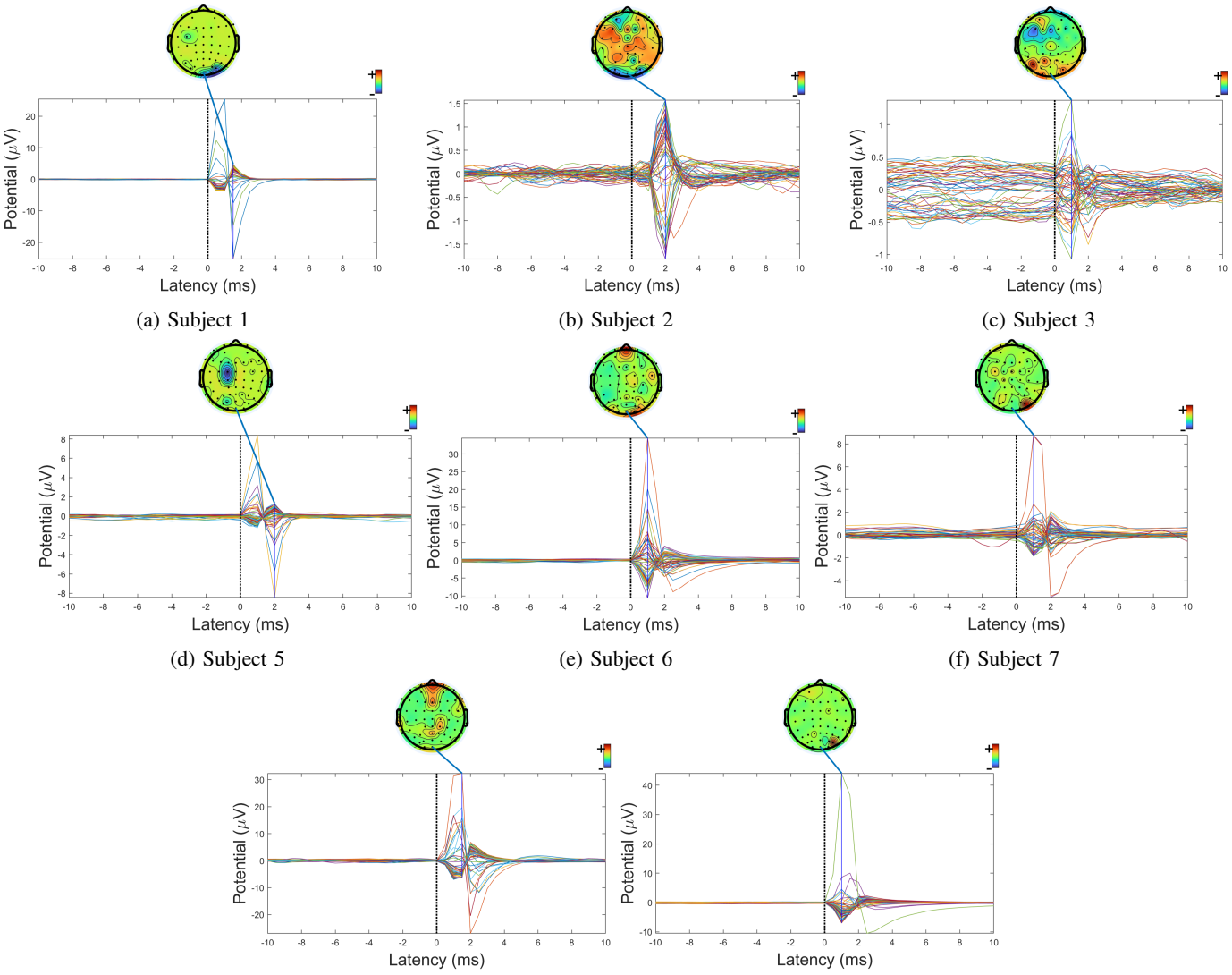

(a) Subject 1 (b) Subject 2 (c) Subject 3

(d) Subject 5 (e) Subject 6 (f) Subject 7

(g) Subject 8 (h) Subject 9

Fig. 19: Electrical artifact. Figures display the average across >4,000 epochs for each subject, and the topography at the time of maximum amplitude. Each line is one channel. The figures show data before removing outlier channels. Latency 0 corresponds to the time of delivery of the electrical stimulation. It must be noted that the value of the vertical axis is different in every figure.

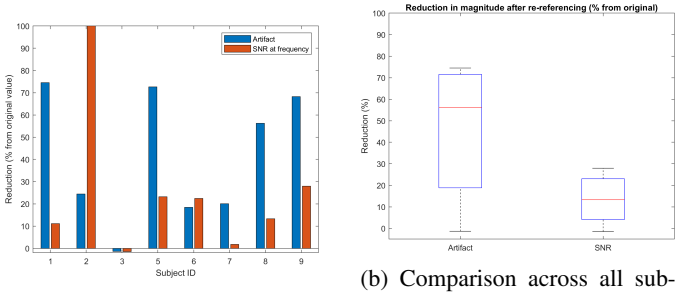

(a) Comparison for each subject. (b) Comparison across all subjects.

Fig. 20: Comparison of the relative decrease in amplitude and SNR for each subject individually and for all subjects. (a) For 5 out of 7 subjects, the relative decrease in SNR was much smaller that the decrease in artifact amplitude. (b) The decrease in SNR was much smaller than the decrease in amplitude. An outlier in SNR with value 689% was excluded from the range of the plot to improve visualization.